UNCLASSIFIED

AD 275 080

Reproduced
by the

ARMED SERVICES TECHNICAL INFORMATION AGENCY
ARLINGTON HALL STATION
ARLINGTON 12, VIRGINIA

UNCLASSIFIED

REPRODUCTION QUALITY NOTICE

This document is the best quality available. The copy furnished to DTIC contained pages that may have the following quality problems:

- Pages smaller or larger than normal.
- Pages with background color or light colored printing.
- Pages with small type or poor printing; and or
- Pages with continuous tone material or color photographs.

Due to various output media available these conditions may or may not cause poor legibility in the microfiche or hardcopy output you receive.

☐ If this block is checked, the copy furnished to DTIC contained pages with color printing, that when reproduced in Black and White, may change detail of the original copy.

BLAST RESPONSE OF A TYPICAL AIRCRAFT FUSELAGE STRUCTURE

R. C. DeHart
N. L. Basdekas

Final Report
Contract NOw-61-0210-C
SwRI Project 1025-3

March 20, 1962

SOUTHWEST RESEARCH INSTITUTE
SAN ANTONIO, TEXAS

SOUTHWEST RESEARCH INSTITUTE
8500 Culebra Road, San Antonio 6, Texas

Department of Structural Research

BLAST RESPONSE OF A TYPICAL AIRCRAFT FUSELAGE STRUCTURE

R. C. DeHart
N. L. Basdekas

Final Report
Contract NOw-61-0210-C
SwRI Project 1025-3

Prepared for

Bureau of Naval Weapons
Department of the Navy
Washington 25, D. C.

March 20, 1962

APPROVED:

Robert C. DeHart

Robert C. DeHart, Director
Department of Structural Research

TABLE OF CONTENTS

LIST OF ILLUSTRATIONS

LIST OF ILLUSTRATIONS (Cont'd)

LIST OF ILLUSTRATIONS (Cont'd)

LIST OF ILLUSTRATIONS

LIST OF TABLES

LIST OF SYMBOLS

A = Cross-sectional area

a = Dimension of the panel in the x-direction, major semi-axis of the elliptical frame

b = Dimension of the panel in the y-direction, minor semi-axis of the elliptical frame, as subscript (bending)

c = Maximum distance of the extreme fibers from the centroid axis of the cross section

D = Flexural rigidity = $\frac{Eh^3}{12(1 - \nu^2)}$

d = As subscript (direct, dynamic)

E = Modulus of elasticity

h = Thickness of panel

I = Second moment of area

i = As subscript (ith mode)

$k_i\ell$ = Solution of the frequency equation

ℓ = Length of stringer

M = Generalized mass, bending moment

m = Number of half-waves in the x-direction

m_i = Mass per unit length or area

N = In-plane force

n = Number of half-waves in the y-direction

P_o = Peak dynamic pressure

LIST OF SYMBOLS (Cont'd)

Q	=	Generalized force
q	=	Generalized coordinate
R	=	Reaction
S	=	Initial tension in the membrane
s	=	Length of circumference, as subscript (of the stringer)
st	=	As subscript (static)
t	=	Time
t_+	=	Duration of the positive phase
V	=	Shear
v	=	Velocity of shock propagation
W	=	Work
w	=	Displacement
$\bar{y}$	=	Maximum distance of the extreme fibers from the centroid of the cross section
α	=	Constant
β	=	Constant
δ	=	Stretching, variation
λ	=	Constant
ν	=	Poisson's ratio
ρ	=	Mass density
σ	=	Stress
ϕ	=	Mode shape
ω	=	Natural frequency

I. INTRODUCTION

In this report, on the basis of elastic dynamic analysis, analytical means have been developed to design a fuselage for a given blast intensity or to determine the maximum blast a given fuselage can withstand. Charts in nondimensional form have been developed determining the critical blast intensity for a given skin size. From the skin's response, the loading on the stringers has been obtained and is given graphically for various values of a nondimensional parameter for peak pressure intensities of P_o = 2 psi and P_o = 1 psi, and their utilization is presented for different skin sizes. The response of the stringers was formulated, and the maximum bending moments produced in a typical stringer for peak pressure intensity of P_o = 2 psi and P_o = 1 psi, for different panel sizes, are presented in convenient graphical form. Also, the stringer's reactions have been obtained for peak pressure intensities of P_o = 2 psi and P_o = 1 psi for different panel sizes and are given in graphical form. An approximate flexural response of the elliptical frame was formulated, and the maximum dynamic stress was determined.

II. ELASTIC DYNAMIC ANALYSIS OF THE FUSELAGE

A. Determination of the Dynamic Response of a Panel Loaded Transversely

The modes of vibration of a plate with fixed-fixed edges and coordinate system shown in Figure 1 can be given by

$$\phi(x, y) = \sum_{m=1,3,5} \sum_{n=1,3,5} \left(1 + \cos \frac{2m\pi x}{a}\right)\left(1 + \cos \frac{2n\pi y}{b}\right) \tag{1}$$

Using energy approach, the frequency of harmonic oscillations was obtained and is given by

$$\omega_{mn}^2 = \frac{17.30D}{m_i} \left[3\left(\frac{m^4}{a^4} + \frac{n^4}{b^4}\right) + \frac{2m^2n^2}{a^2b^2}\right] \tag{2}$$

where a and b are the dimensions of the skin panel, D the flexural rigidity of the skin and m_i is the mass per unit of skin area.

In the case of forced vibrations, the generalized coordinates satisfy the differential equation

$$\ddot{q}_{mn} + \omega_{mn}^2 q_{mn} = \frac{Q_{mn}(t)}{M_{mn}} \tag{3}$$

where M_{mn}, the generalized mass is given by

$$M_{mn} = m_i \int_{-a/2}^{a/2} \int_{-b/2}^{b/2} \phi_{mn}^2(x, y)\, dxdy \tag{4}$$

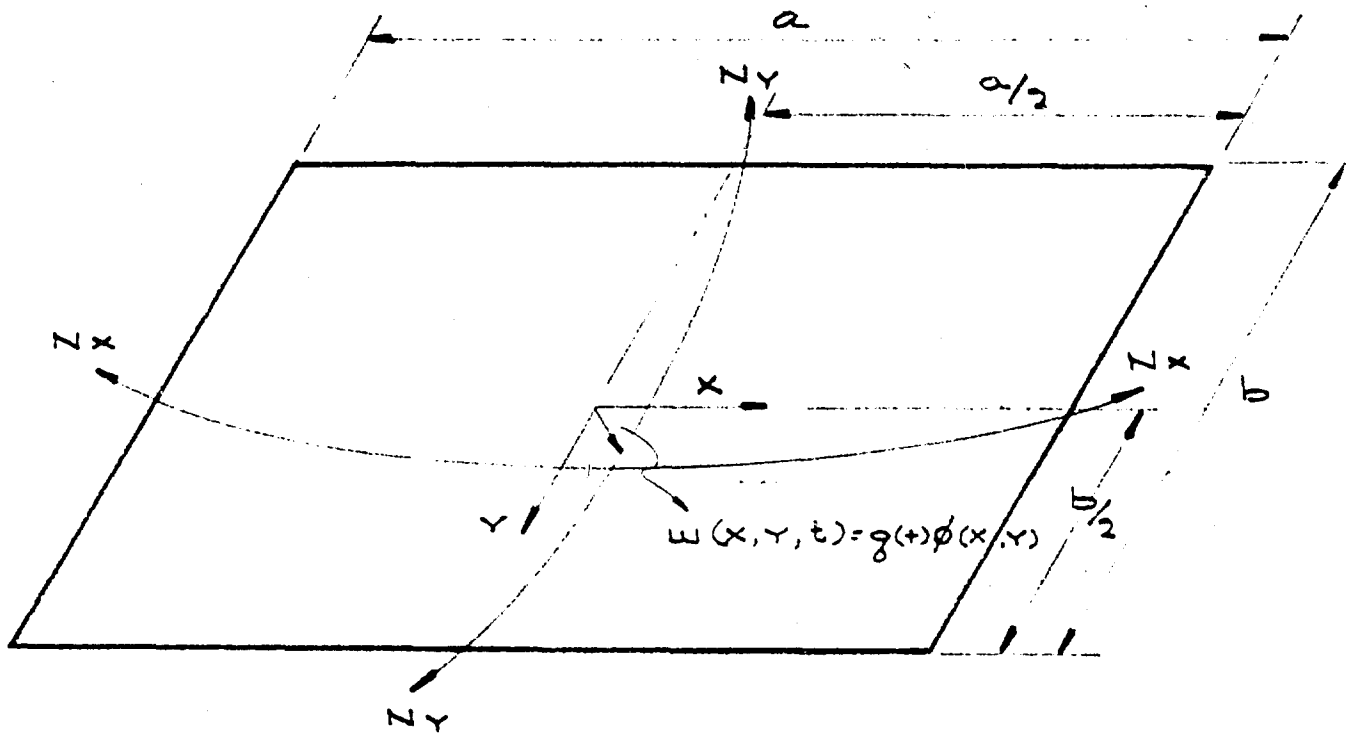

FIGURE 1. PANEL CONSIDERED WITH LOADING IN ITS OWN PLANE

When the distance between the supports of the panel is fixed, the in-plane forces develop. Using virtual work, the following expression is obtained

$$Q_{mn}\delta q_{mn} = \delta W_{mn}$$

where $Q_{mn}(t)$ is the generalized force in the m, n mode, q_{mn} is the generalized displacement in the m, n mode, W_{mn} is the work done by the loading in the m, n mode and δ stands for variation.

Then

$$\delta W_{mn} = \delta \int_{-a/2}^{a/2} \int_{-b/2}^{b/2} P(x, y, t) w_{mn}(x, y, t) dx dy$$

$$- \delta \int_{-b/2}^{b/2} \left[\frac{1}{2} N_x \delta_x\right] dy - \delta \int_{-a/2}^{a/2} \left[\frac{1}{2} N_y \delta_y\right] dx$$

where

$P(x, y, t)$ is the transverse loading

$w_{mn}(x, y, t)$ is the transverse dynamic displacement of the panel

N_x is the force developed at the edge due to stretching δ_x in the x-direction

N_y is the force developed at the edge due to stretching δ_y in the y-direction

but

$$\delta_x = \frac{1}{2} \int_{-a/2}^{a/2} \left(\frac{\partial w_{mn}}{\partial x}\right)^2 dx; \quad \delta_y = \frac{1}{2} \int_{-b/2}^{b/2} \left(\frac{\partial w_{mn}}{\partial y}\right)^2 dy$$

and

$$N_x = \frac{\delta_x}{a} Eh ; \qquad N_y = \frac{\delta_y}{b} Eh$$

Then

$$\delta W_{mn} = \delta \int_{-a/2}^{a/2} \int_{-b/2}^{b/2} P(x, y, t) w_{mn}(x, y, t) dxdy$$

$$- \delta \int_{-b/2}^{b/2} \left[\frac{Eh}{8a} \int_{-a/2}^{a/2} \left(\frac{\partial w_{mn}}{\partial x} \right)^2 dx \cdot \int_{-a/2}^{a/2} \left(\frac{\partial w_{mn}}{\partial x} \right)^2 dx \right] dy$$

$$- \delta \int_{-a/2}^{a/2} \left[\frac{Eh}{8b} \int_{-b/2}^{b/2} \left(\frac{\partial w_{mn}}{\partial y} \right)^2 dy \cdot \int_{-b/2}^{b/2} \left(\frac{\partial w_{mn}}{\partial y} \right)^2 dy \right] dx$$

but

$$w_{mn}(x, y, t) = q_{mn}(t) \phi_{mn}(x, y)$$

Then

$$\delta W_{mn} = \delta q_{mn}(t) \left\{ \int_{-a/2}^{a/2} \int_{-b/2}^{b/2} P(x, y, t) \phi_{mn}(x, y) dxdy \right.$$

$$- \frac{Eh}{2a} q_{mn}^3(t) \int_{-b/2}^{b/2} \left[\int_{-a/2}^{a/2} \left(\frac{\partial \phi_{mn}}{\partial x} \right)^2 dx \cdot \int_{-a/2}^{a/2} \left(\frac{\partial \phi_{mn}}{\partial x} \right)^2 dx \right] dy$$

$$\left. - \frac{Eh}{2b} q_{mn}^3(t) \int_{-a/2}^{a/2} \left[\int_{-b/2}^{b/2} \left(\frac{\partial \phi_{mn}}{\partial y} \right)^2 dy \cdot \int_{-b/2}^{b/2} \left(\frac{\partial \phi_{mn}}{\partial y} \right)^2 dy \right] dx \right\}$$

but

$$Q_{mn}\delta q_{mn} = \delta W_{mn}$$

Then

$$Q_{mn}(t) = \int_{-a/2}^{a/2}\int_{-b/2}^{b/2} P(x, y, t)\phi_{mn}(x, y)\,dxdy$$

$$-\left\{\frac{Eh}{2a}\int_{-b/2}^{b/2}\left[\int_{-a/2}^{a/2}\left(\frac{\partial\phi_{mn}}{\partial x}\right)^2 dx \cdot \int_{-a/2}^{a/2}\left(\frac{\partial\phi_{mn}}{\partial x}\right)^2 dx\right] dy\right.$$

$$\left.+\frac{Eh}{2b}\int_{-a/2}^{a/2}\left[\int_{-b/2}^{b/2}\left(\frac{\partial\phi_{mn}}{\partial y}\right)^2 dy \cdot \int_{-b/2}^{b/2}\left(\frac{\partial\phi_{mn}}{\partial y}\right)^2 dy\right] dx\right\} q_{mn}^3(t) \tag{5}$$

In the case under consideration

$$\phi_{mn}(x, y) = \left(1 + \cos\frac{2m\pi x}{a}\right)\left(1 + \cos\frac{2n\pi y}{b}\right)$$

and the $Q_{mn}(t)$ is given by

$$Q_{mn}(t) = \int_{-a/2}^{a/2}\int_{-b/2}^{b/2} P(x, y, t)\phi_{mn}(x, y)dxdy - \frac{Ehab}{2}\left[\left(\frac{2m\pi}{a}\right)^4\right.$$

$$\left.+\left(\frac{2n\pi}{b}\right)^4\right] q_{mn}^3(t) \tag{6}$$

B. Determination of the Sensitivity of Panel Response to the Manner in Which the Panel is Loaded

The shock is travelling across the panel as shown in Figure 2, and the loading is given by

$$P(x, t) = P_o\left(1 - \frac{t - \frac{a/2 + x}{v}}{t_+}\right)$$

where

P_o = Peak pressure

t = Time

a = Dimension of panel in the x-direction

v = Velocity of shock propagation

t_+ = Duration of the positive phase

Using the above $P(x, t)$, the generalized force is given by

$$Q_{mn}(t) = P_o\left[\left(1 - \frac{t}{t_+}\right) + \frac{a}{2vt_+}\right] ab - \frac{Ehab}{2}\left[\left(\frac{2m\pi}{a}\right)^4 + \left(\frac{2n\pi}{b}\right)^4\right] q_{mn}^3(t) \qquad (7)$$

The differential equation for the generalized displacement q_{mn} is

$$\ddot{q}_{mn} + \omega_{mn}^2 q_{mn} = \frac{Q_{mn}(t)}{M_{mn}}$$

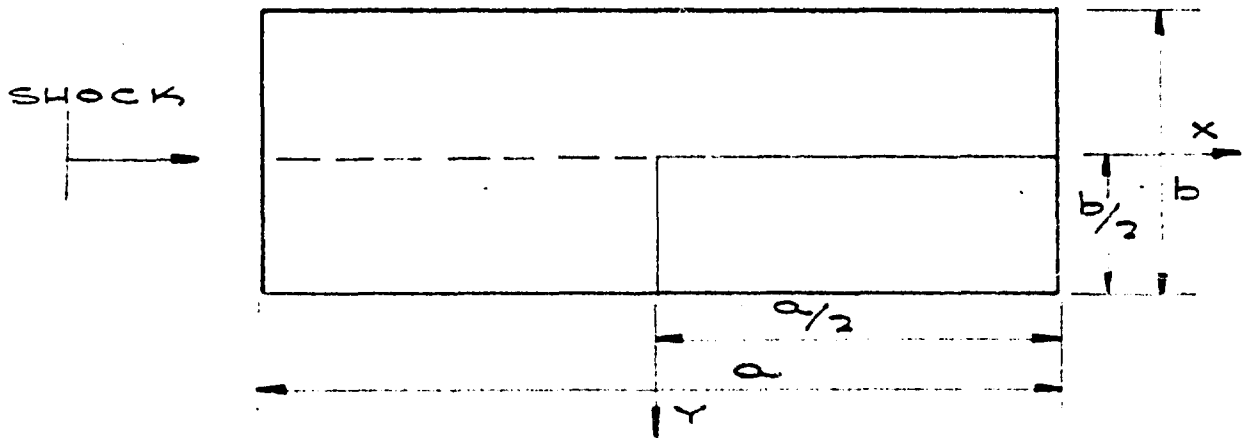

FIGURE 2. PANEL AND DIRECTION OF SHOCK PROPAGATION

where

ω_{mn} is the natural frequency of the panel in the m, n mode

$Q_{mn}(t)$ is the generalized force in the m, n mode

M_{mn} is the generalized mass in the m, n mode

For the case under consideration

$$\omega_{mn}^2 = \frac{17.30D}{m_i}\left[3\left(\frac{m^4}{a^4} + \frac{n^4}{b^4}\right) + \frac{2m^2n^2}{a^2b^2}\right]$$

where

$$D = \frac{Eh^3}{12(1 - \nu^2)}$$

h = Thickness of the panel

E = Modulus of elasticity of the panel material

ν = Poisson's ratio

m and n number of half waves in the x- and y-directions respectively

m_i = Mass per unit area of panel

$$M_{mn} = m_i \int_{-a/2}^{a/2} \int_{-b/2}^{b/2} \phi_{mn}^2(x, y)\, dx = 2.25\, m_i ab \qquad (8)$$

The $\ddot{q}_{mn}(t_i)$ in terms of differences is given by

$$\ddot{q}_{mn}(t_i) = \frac{q_{mn}(t_i + 1) - 2q_{mn}(t_i) + q_{mn}(t_i - 1)}{(\Delta t)^2}$$

where Δt = time interval

Substituting $\ddot{q}_{mn}(t_i)$, in terms of differences, in the differential equation and solving for $q_{mn}(t_i + 1)$ the following difference equation is obtained

$$q_{mn}(t_i + 1) = A(t_i) + B_{mn}q^3_{mn}(t_i) + C_{mn}q_{mn}(t_i) - q_{mn}(t_i - 1) \qquad (9)$$

where

$$A(t_i) = \frac{(\Delta t)^2 P_o}{2.25 m_i}\left[\left(1 - \frac{t_i}{t_+}\right) + \frac{a}{2vt_+}\right]$$

$$B_{mn} = -\frac{Eh(\Delta t)^2}{4.5 m_i}\left[\left(\frac{2m\pi}{a}\right)^4 + \left(\frac{2n\pi}{b}\right)^4\right]$$

$$C_{mn} = -\omega^2_{mn}(\Delta t)^2 + 2$$

Considering the loading only as a function of time then

$$P(t) = P_o\left(1 - \frac{t}{t_+}\right)$$

and the $q_{mn}(t_i + 1)$ is given by

$$q_{mn}(t_i + 1) = A(t_i) + B_{mn}q^3_{mn}(t_i) + C_{mn}q_{mn}(t_i) - q_{mn}(t_i - 1)$$

where

$$A(t_i) = \frac{(\Delta t)^2 P_o}{2.25 m_i}\left(1 - \frac{t}{t_+}\right)$$

and the B_{mn} and C_{mn} are the same as in the previous case.

The following typical case has been considered

$v = 1000$ ft/sec

$t_+ = 1$ sec

$P_o = 1$ psi

$a = 20''$

$b = 8''$

$h = 0.03''$

$E = 10.6 \times 10^6$ (Aluminum)

$\nu = 0.3$

$\Delta t = 0.0002$ sec

and

$q_{mn}(0) = \dot{q}_{mn}(0)$; (rest initial conditions)

Since the 1, 1 mode is the predominant one, $q_{11}(t)$ was computed for the two types of loading and the results obtained are given in the table below.

Loading	$q_{11\ max}$	Time of $q_{11\ max}$, sec	%
P(x, t)	374.23×10^{-4}	0.0012	1.00019
P(t)	374.16×10^{-4}	0.0012	

In the light of the above results, q_{11}, which is a measure of response is essentially identical for both loading cases, not only in terms

of magnitude but also in terms of time dependency. Thus, in the remainder of the work, the loading will be taken as a function of time only.

In order to see how the $q_{11\ max}(t)$ varies as the peak load intensity varies, the response of the previously considered panel was determined for P_o of 2 psi and 4 psi. The $q_{11\ max}(t)$ were determined and are given in Figure 3. The nonlinearity is clearly shown, and the time of maximum generalized displacement which is the same as the time at which q_{11} is maximum, as expected, becomes smaller and smaller with increase of peak load intensity.

C. Linear Panel Response

In case the stretching of the middle plane of the panel is neglected, the nonlinearity is removed and the difference equation becomes

$$q_{mn}(t_i + 1) = A(t_i) + C_{mn}q_{mn}(t_i) - q_{mn}(t_i - 1) \tag{10}$$

The same panel has been considered as before with $P_o = 0.1$ psi and initial conditions corresponding to no motion. The maximum $q_{11}(t)$ and the time it occurred are given in Figure 3. By comparing the results of B and C as given in Figure 3, it is clear that the greater the P_o (peak load intensity) becomes, the greater the reduction factor in maximum displacement becomes when stretching of the panel is taken into account. When membrane forces are neglected, the relation of $q_{11\ max}$ and P_o is linear:

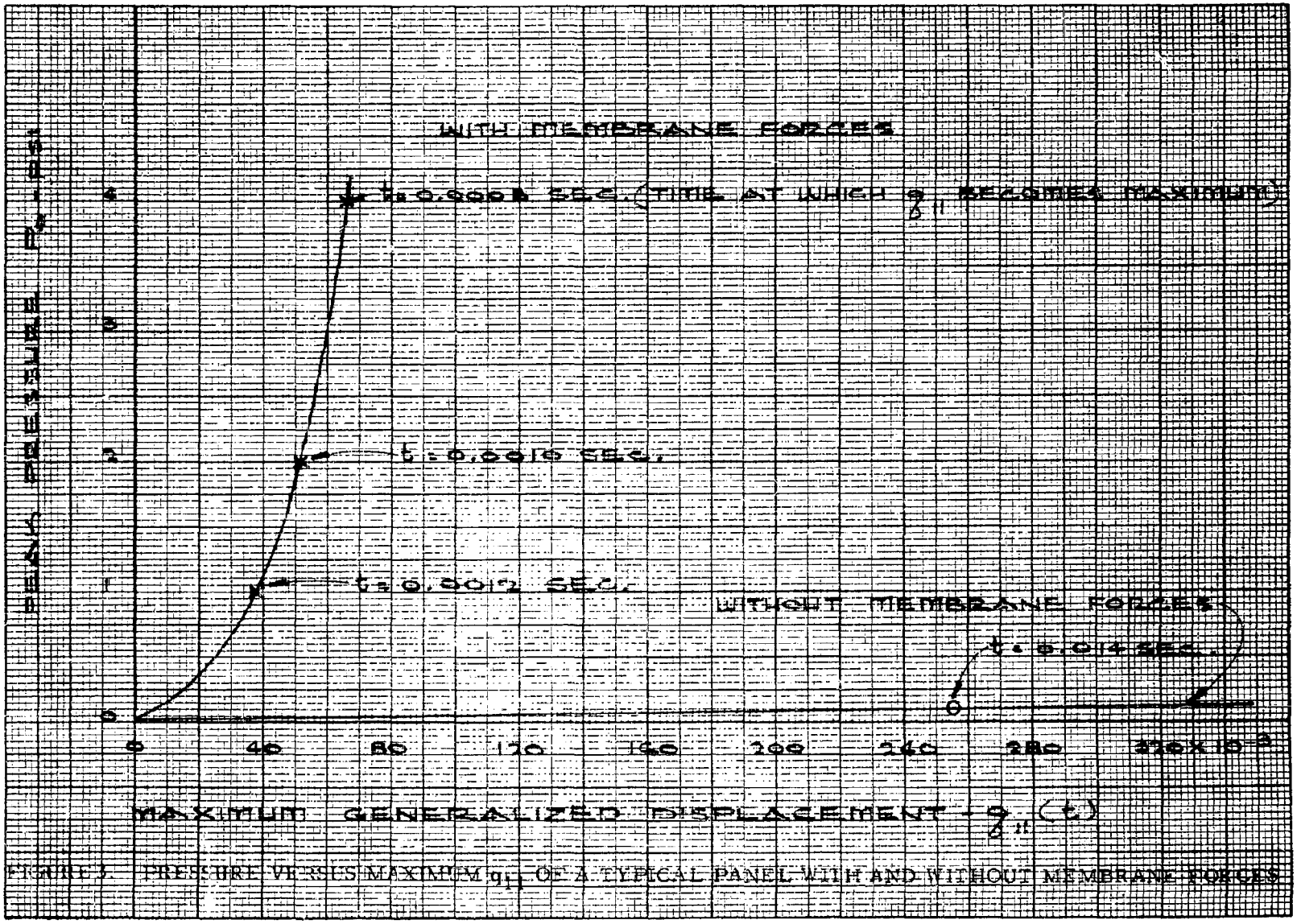

FIGURE 5 PRESSURE VERSUS MAXIMUM q_{11} OF A TYPICAL PANEL WITH AND WITHOUT MEMBRANE FORCES

$$\frac{P'_o}{P^*_o} = \frac{q'_{11\ max}}{q^*_{11\ max}}$$

When the membrane forces are included, the P_o vs $q_{11}(t)_{max}$ is not linear and approaches the relation

$$\sqrt{\frac{P'_o}{P^*_o}} = \frac{q'_{11\ max}}{q^*_{11\ max}}$$

D. Determination of Maximum Direct and Bending Stress

Utilizing the strain-displacement and stress-strain relations, the maximum direct stress in the panel is given by

$$\sigma_d = \frac{8\pi^2 E}{b^2} \sum_m \sum_n n^2 q^2_{mn}(t) \tag{11}$$

and the bending stress at $x = 0$, $y = \frac{b}{2}$ is given by

$$\sigma_b = - \frac{8\pi^2 E h^3}{12(1-\nu^2)} \left[\frac{1}{b^2} \sum_m \sum_n n^2 q_{mn}(t) \right] \tag{12}$$

The $q_{11}(t)$ is the predominant component and using only this component, the ratio $\left|\frac{\sigma_d}{\sigma_b}\right|$ is equal to $\left|\frac{\sigma_d}{\sigma_b}\right| = \left|\frac{12(1-\nu^2)q_{11}}{h^3}\right|_{\nu=0.3} = \frac{10.9 q_{11}}{h^3}$

For the typical case considered in B, the $h = 0.03''$ and the $q_{11\ max}$ for $P_o = 1$ psi was found equal to about 374.24×10^{-4}. For this case:

$$\left|\frac{\sigma_d}{\sigma_b}\right| = \frac{10.9 \times 374.24 \times 10^{-4}}{(0.03)^3} = \frac{10.9 \times 374.24 \times 10^{-4}}{27 \times 10^{-6}} = 15,100$$

Even if h = 0.05" and say $q_{11\ max}$ drops to 37×10^{-4}, then the

$$\left|\frac{\sigma_d}{\sigma_b}\right| = \frac{10.9 \times 37 \times 10^{-4}}{(0.05)^3} = 322$$

E. Simplification of the Procedure for Determining Panel Response

On the basis of the above results, it is clear that when the in-plane forces are taken into account the panel behaves primarily like a membrane, which is equivalent to saying that the bending stresses are insignificant, and the panel can be considered as simply supported with the distance between its supports fixed. Thus, for the cases to be treated in the future, the panel will be considered as a membrane, and the stretching of the middle plane will be taken into consideration. The above simplification will result in simplification of the computation work without any important loss of accuracy.

F. Response of the Panel and Resulting Stresses

1. Forced Vibrations of a Membrane With Fixed Distance of Its Edges

The coordinate system considered is given in Figure 4.

The dynamic displacement of the membrane can be represented by

$$w(x, y, t) = \Sigma\Sigma q_{mn}(t)\phi_{mn}(x, y)$$

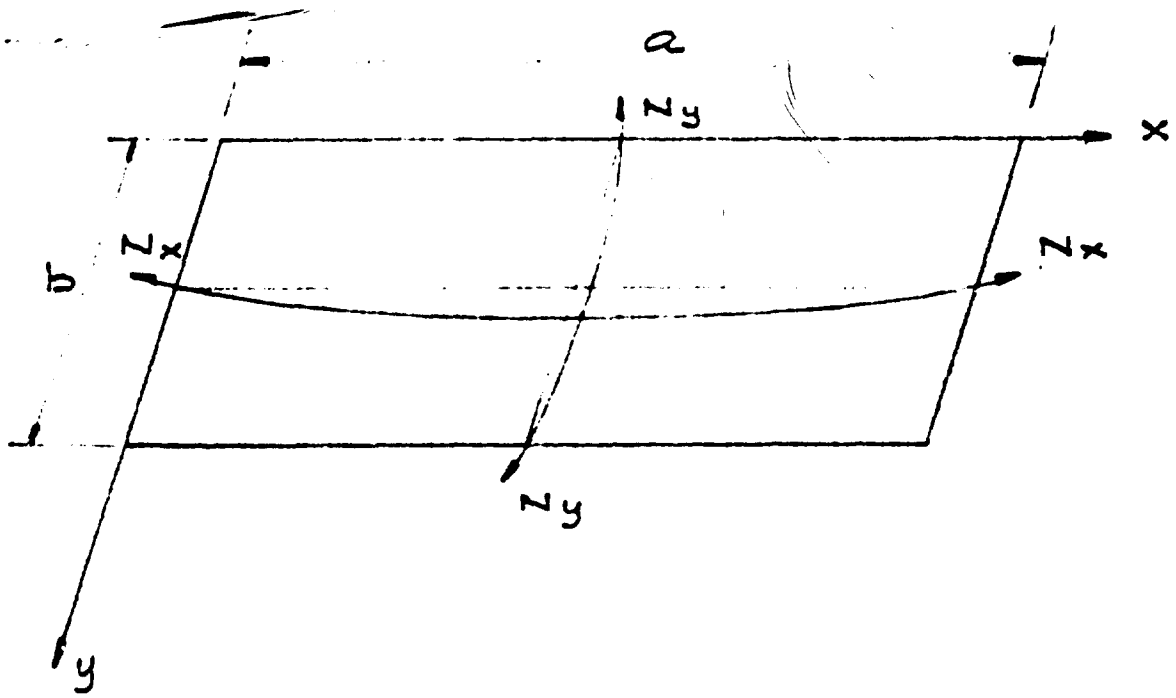

FIGURE 4. COORDINATE SYSTEM OF THE PANEL

where $\phi_{mn}(x, y)$ are the modes of free vibration of the membrane and are given by

$$\phi_{mn}(x, y) = \sin \frac{m\pi x}{a} \sin \frac{n\pi y}{b} \tag{13}$$

and $q_{mn}(t)$ satisfy the differential equation

$$\ddot{q}_{mn} + \omega_{mn}^2 q_{mn} = \frac{Q_{mn}}{M_{mn}} \tag{14}$$

where

$$\omega_{mn}^2 = \frac{S\pi^2}{m_i} \left(\frac{m^2}{a^2} + \frac{n^2}{b^2} \right) \tag{15}$$

S = Initial tension of the membrane

m_i = Mass per unit area of the membrane

Q_{mn} = Generalized force which is given by

$$Q_{mn}(t) = \int_0^a \int_0^b P(x, y, t)\, \phi_{mn}(x, y)\, dxdy$$

$$- \frac{Eh}{2a} q_{mn}^3(t) \int_0^b \left[\int_0^a \left(\frac{\partial \phi_{mn}}{\partial x} \right)^2 dx \int_0^a \left(\frac{\partial \phi_{mn}}{\partial x} \right)^2 dx \right] dy \tag{16}$$

$$- \frac{Eh}{2b} q_{mn}^3(t) \int_0^a \left[\int_0^b \left(\frac{\partial \phi_{mn}}{\partial y} \right)^2 dy \int_0^b \left(\frac{\partial \phi_{mn}}{\partial y} \right)^2 dy \right] dx$$

and

$$M_{mn} = m_i \int_0^a \int_0^b \phi_{mn}^2(x, y)\, dxdy \tag{17}$$

The $Q_{mn}(t)$ and M_{mn} for the $\phi_{mn}(x, y)$ under consideration are given below.

$$\text{The } \int_0^a \int_0^b P(x, y, t)\phi_{mn}(x, y)\, dxdy \Bigg|_{P(x, y, t) = P(t)} =$$

$$= P(t) \int_0^a \int_0^b \sin \frac{m\pi x}{a} \sin \frac{n\pi y}{b}\, dxdy = P(t) \frac{ab}{mn\pi^2} (1 - \cos m\pi)(1 - \cos n\pi)$$

For $P(t) = P_o \left(1 - \frac{t}{t_+}\right)$

Then

$$\int_0^a \int_0^b P(t)\phi_{mn}(x, y)dxdy = \frac{P_o ab}{mn\pi^2} (1 - \cos m\pi)(1 - \cos n\pi)\left(1 - \frac{t}{t_+}\right)$$

but for m and/or n even, the $\int_0^a \int_0^b P(t)\phi_{mn}(x, t)\, dxdy = 0$

$$\therefore \int_0^a \int_0^b P(t)\phi_{mn}(x, y)\, dxdy = \frac{4abP_o}{mn\pi^2} \left(1 - \frac{t}{t_+}\right) \Bigg|_{m, n = \text{odd}}$$

Proceeding in a similar way, the other integrals of (16) are computed, and finally the generalized force is given by:

$$Q_{mn}\Big|_{m,\,n=\text{odd}} = \frac{4abP_o}{mn\pi^2}\left(1 - \frac{t}{t_+}\right) - \frac{3\pi^4}{64}\,Ehab\left[\frac{m^4}{a^4} + \frac{n^4}{b^4}\right] q_{mn}^3(t)$$

or

$$Q_{mn}\Big|_{m,\,n=\text{odd}} = \frac{0.406abP_o}{mn}\left(1 - \frac{t}{t_+}\right) - 4.55\,Ehab\left[\frac{m^4}{a^4} + \frac{n^4}{b^4}\right] q_{mn}^3(t) \quad (18)$$

The generalized mass is given by

$$M_{mn} = m_i \int_0^a \int_0^b \phi_{mn}^2(x, y)\,dxdy = m_i \int_0^a \int_0^b \sin^2\frac{m\pi x}{a} \sin^2\frac{n\pi x}{b}\,dxdy$$

$$= \frac{m_i ab}{4}$$

or

$$M_{mn} = 0.25\,m_i ab \quad (19)$$

For S (Initial Tension of the Membrane) = 0

Equation (15) yields $\omega_{mn} = 0$, and the Equation (14) becomes

$$\ddot{q}_{mn}(t) = \frac{Q_{mn}}{M_{mn}} \quad (20)$$

In terms of differences

$$\ddot{q}_{mn}(t) = \frac{q_{mn}(t_i - 1) - 2q_{mn}(t_i) + q_{mn}(t_i + 1)}{(\Delta t)^2}$$

and Equation (20) reduces to

$$\frac{q_{mn}(t_i - 1) - 2q_{mn}(t_i) + q_{mn}(t_i + 1)}{(\Delta t)^2} = \frac{\frac{0.406abP_o}{mn}\left(1 - \frac{t}{t_+}\right) - 4.55Ehab\left[\frac{m^4}{a^4} + \frac{n^4}{b^4}\right] q^3_{mn}(t_i)}{0.25m_iab}$$

or

$$q_{mn}(t_i + 1) = 2q_{mn}(t_i) + A_{mn}(t_i) + B_{mn}q^3_{mn}(t_i) - q_{mn}(t_i - 1) \qquad (21)$$

where

$$A_{mn}(t_i) = \frac{1.624(\Delta t)^2 P_o}{m_i mn}\left(1 - \frac{t_i}{t_+}\right)$$

$$B_{mn} = -\frac{18.20Eh(\Delta t)^2}{m_i}\left[\frac{m^4}{a^4} + \frac{n^4}{b^4}\right]$$

2. Determination of the Maximum Stress in the Panel

The in-plane forces N_x and N_y, as shown in Figure 4, are given by

$$N_{xmn} = \frac{\delta x}{a} Eh = \frac{Eh}{a} 1/2 \int_0^a \left(\frac{\partial \phi_{mn}}{\partial x}\right)^2 dx \qquad (22)$$

Using $\phi_{mn}(x, y)$, the expression given by Equation (13), the (22) becomes

$$N_{xmn} = \frac{Eh}{4}\left(\frac{m\pi}{a}\right)^2 \sin^2 \frac{n\pi y}{b} q^2_{mn}(t)$$

and the stress due to N_{xmn} is given by

$$\sigma_{xmn}\Big|_{max} = \frac{N_{xmn}}{h}\Big|_{max} = \frac{E}{4}\left(\frac{m\pi}{a}\right)^2 q_{mn}^2(t)\Big|_{max}$$

The same way

$$\sigma_{ymn}\Big|_{max} = \frac{N_{ymn}}{h}\Big|_{max} = \frac{E}{4}\left(\frac{n\pi}{b}\right)^2 q_{mn}^2(t)\Big|_{max}$$

The maximum stress takes place in the shorter direction and it is equal to

$$\sigma_{mn\,max} = \sigma_{mn}\Big|_{x=a/2} = \frac{E}{4}\left(\frac{n\pi}{b}\right)^2 q_{mn}^2(t)\Big|_{max} = 2.46E\left(\frac{n}{b}\right)^2 q_{mn}^2(t)\Big|_{max}$$

$$\therefore \sigma_{max} = \left\{\Sigma\Sigma\, 2.46E\left(\frac{n}{b}\right)^2 q_{mn}^2(t)\right\}_{max} \qquad (23)$$

Using Equation (21), the response of the panels was determined, and, employing Equation (23), the maximum stresses were obtained and are given in nondimensional form in Figure 5.

G. Determination of the Load on the Stringer

According to Figure 4, the reaction at $x = 0$ is

$$R\Big|_{x=0} = N_{xmn}\frac{\partial\phi_{mn}}{\partial x}\Big|_{x=0} q_{mn}(t)$$

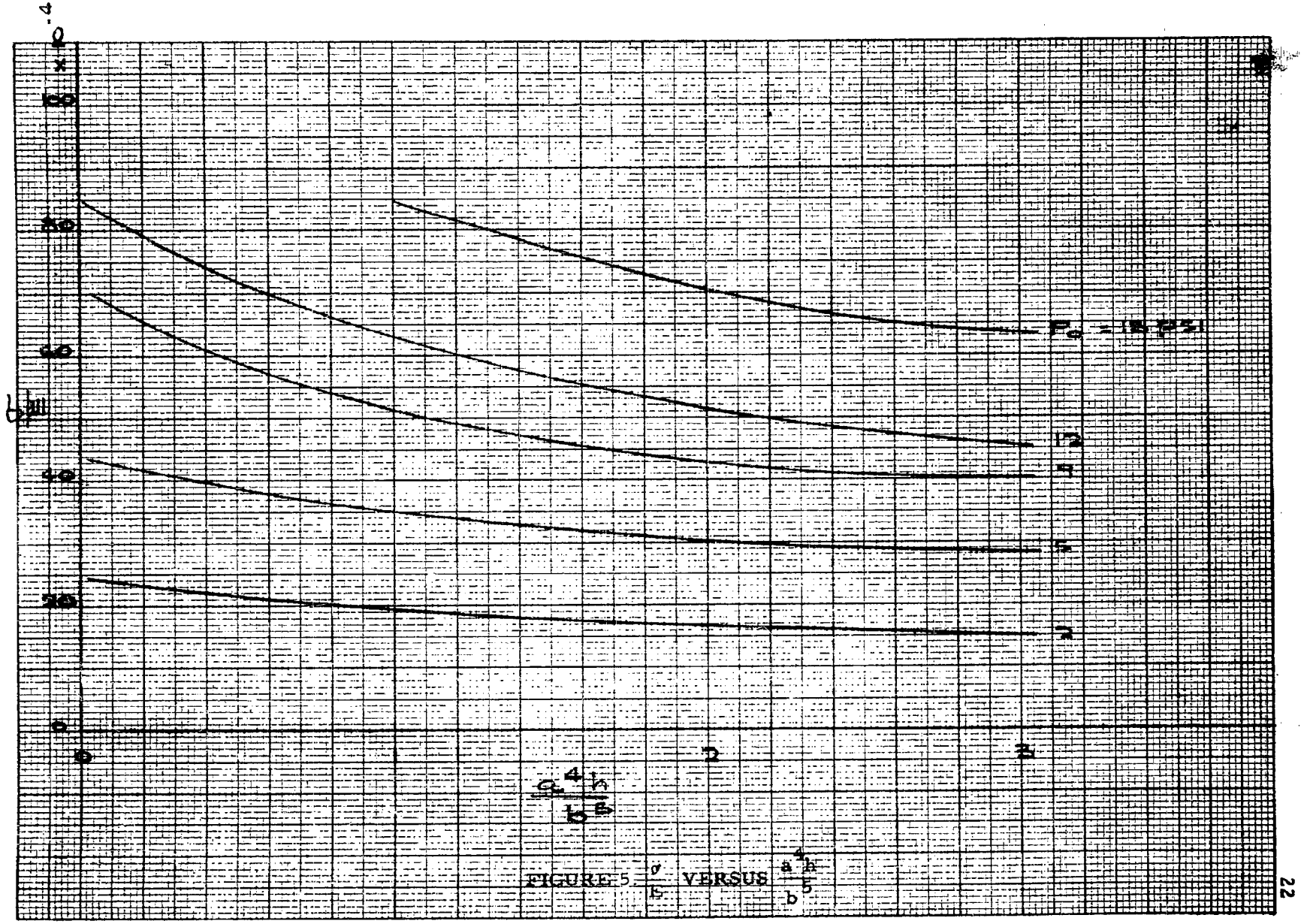

FIGURE 5 $\frac{\sigma}{E}$ VERSUS $\frac{a}{b}\sqrt[4]{\frac{h}{b}}$

but

$$N_{xmn}\ \frac{Eh}{4}\left(\frac{m\pi}{a}\right)^2 \sin^2\frac{n\pi y}{b}\ q_{mn}^2(t)$$

and

$$\left.\frac{\partial \phi_m}{\partial x}\right|_{x=0} = \left(\frac{m\pi}{a}\right)\cos\frac{m\pi x}{a}\sin\frac{n\pi y}{b}\Bigg|_{x=0} = \left(\frac{m\pi}{a}\right)\sin\frac{n\pi y}{b}$$

or

$$R\Big|_{x=0} = \sum\sum \frac{Eh}{4}\left(\frac{m\pi}{a}\right)^3 \sin^3\frac{n\pi y}{b}\ q_{mn}^3(t) =$$

$$= \Sigma\Sigma\, 7.74Eh\left(\frac{m}{a}\right)^3 \sin^3\frac{n\pi y}{b}\ q_{mn}^3(t) \qquad (24)$$

The same way the $R\Big|_{y=0}$, which is the loading on the stringer, is obtained and is given by

$$R\Big|_{y=0} = \Sigma\Sigma\, 7.74Eh\left(\frac{n}{b}\right)^3 \sin^3\frac{m\pi x}{a}\ q_{mn}^3(t) \qquad (25)$$

The

$$R\Big|_{y=0\ max} = \Sigma\Sigma 7.74Eh\left(\frac{n}{b}\right)^3 q_{mn}^3(t)$$

In order to obtain the relative contribution of the q_{mn} to the $R\Big|_{y=0\ max}$, a typical panel was considered (a = 20", b = 8"; h = 0.03"), and subjected

to a linearly decaying dynamic load of peak intensity equal to P_o = 1 psi, and the q_{mn} were determined when q_{11} reached its maximum value. Their magnitudes are

$$q_{11} = 0.1619$$

$$q_{13} = 0.0005$$

$$q_{31} = 0.0266$$

$$q_{33} = 0.0183$$

Their contribution to the $R\big|_{y=0\ max}$ is

$$q_{11}^3 = 4,250 \times 10^{-6}$$

$$(3)^3 q_{13}^3 \approx 0$$

$$q_{13}^3 = 18.8 \times 10^{-6}$$

$$(3)^3 q_{33}^3 = \frac{56 \times 10^{-6}}{4,324.8 \times 10^{-6}}$$

It is clearly shown that the contribution of the q_{11} alone is 98.3% of the total magnitude. On the above basis, the loading of the stringer will be approximated by the contribution of the $q_{11}(t)$ alone, and thus will be given by

$$R\Big|_{y=0} = \frac{7.74Eh}{b^3} \sin^3 \frac{\pi x}{a}\, q_{11}^3(t) \tag{26}$$

In order to get an idea how the $q_{11}^3(t)$ varies with time, the $q_{11}^3(t)$ has been plotted, for the typical panel considered previously, and is given in Figure 6.

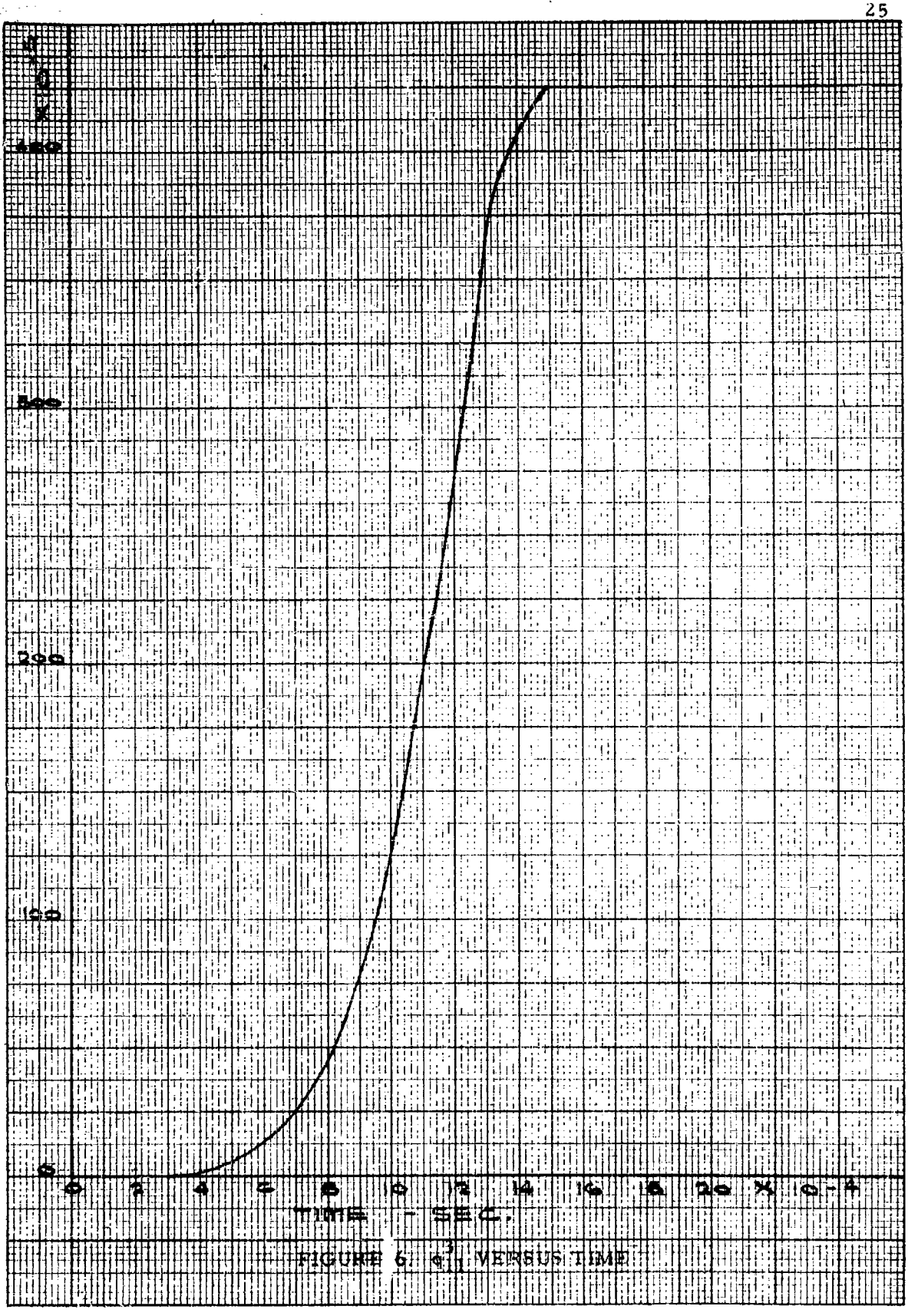

FIGURE 6 ϕ_{11}' VERSUS TIME

H. Formulation of the Stringer's Response

The stringers will be considered as fixed-end beams, as shown in Figure 7. The modes of free vibrations are given by

$$\phi_i(x) = \lambda_i(\cos k_i x - \text{ch } k_i x) + (\sin k_i x - \text{sh } k_i x) \tag{27}$$

where

$$\lambda_i = -\frac{(\sin k_i \ell - \text{sh } k_i \ell)}{(\cos k_i \ell - \text{ch } k_i \ell)} \tag{28}$$

and

$$k_1 \ell = 4.730$$

$$k_2 \ell = 7.853$$

$$k_3 \ell = 10.996$$

$$k_4 \ell = 14.137$$

$$k_5 \ell = 17.279$$

In the case of forced vibrations, the generalized coordinates satisfy the differential equation

$$\ddot{q}_i(t) + \omega_i^2 q_i(t) = \frac{Q_i(t)}{M_i} \tag{29}$$

where

$$\omega_i = (k_i)^2 \sqrt{\frac{EI}{m_i}} = \text{Frequency of free vibrations}$$

$$Q_i(t) = \int_0^{\ell} \phi_i(x) P(x, t)\, dx = \text{Generalized force}$$

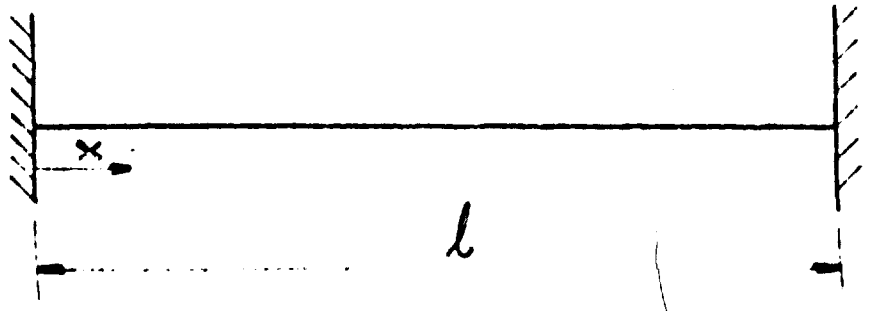

FIGURE 7. COORDINATE SYSTEM AND BOUNDARY CONDITIONS USED FOR THE STRINGER

$$M_i = m_i \int_0^{\ell} \phi_i^2(x)\,dx = \text{Generalized mass}$$

m_i = Mass per unit length of stringer

The generalized force is

$$Q_i(t) = \int_0^{\ell} \phi_i(x)\,P(x,t)\,dx$$

where P(x, t) is given by Equation (26) and is

$$P(x,t) = \frac{7.74Eh}{b^3} \sin^3 \frac{\pi x}{a}\, q_{11}^3(t)$$

or

$$Q_i(t) = \frac{7.74Eh}{b^3}\, q_{11}^3(t) \int_0^{\ell} [\lambda_i(\cos k_i x - \text{ch}\, k_i x) + (\sin k_i x - \text{sh}\, k_i x)] \sin^3 \frac{\pi x}{a}\,dx$$

After performing the integration, the $Q_i(t)$ can be given as

$$Q_i(t) = \frac{7.74Eh}{b^3}\, a\beta_i q_{11}^3(t) \tag{30}$$

where

$$\beta_i = \left\{ -\frac{3\pi}{4}\left[\frac{1}{(k_i a)^2 + \pi^2} - \frac{1}{(k_i a)^2 + (3\pi)^2}\right] \cdot \left[\text{sh}\, k_i a + \lambda_i(\text{ch}\, k_i a + 1)\right] + \right.$$

$$+ \lambda_i \left[3/4 \left(\frac{1 - \cos(\pi - k_i a)}{2(\pi - k_i a)} + \frac{1 - \cos(\pi + k_i a)}{2(\pi + k_i a)} \right) - 1/4 \left(\frac{1 - \cos(3\pi - k_i a)}{2(3\pi - k_i a)} + \frac{1 - \cos(3\pi + k_i a)}{2(3\pi + k_i a)} \right) \right] +$$

$$\left. + \left[3/4 \left(\frac{\sin(\pi - k_i a)}{2(\pi - k_i a)} - \frac{\sin(\pi + k_i a)}{2(\pi + k_i a)} \right) - 1/4 \left(\frac{\sin(3\pi - k_i a)}{2(3\pi - k_i a)} - \frac{\sin(3\pi + k_i a)}{2(3\pi + k_i a)} \right) \right] \right\} \tag{31}$$

The generalized mass is given by $M_i = m_i \int_0^{\ell} \phi_i^2(x)\, dx$

or

$$M_i = m_i \int_0^{\ell} [\lambda_i(\cos k_i x - \text{ch}\, k_i x) + (\sin k_i x - \text{sh}\, k_i x)]^2\, dx$$

After performing the integration, the M_i can be written as

$$M_i = m_i \ell a_i \tag{32}$$

where

$$a_i = \frac{1}{2k_i\ell} [\lambda^2(2k_i\ell + \sin k_i\ell \cos k_i\ell + \text{sh}\, k_i\ell\, \text{ch}\, k_i\ell - 2\, \text{sh}\, k_i\ell \cos k_i\ell - 2\text{ch}\, k_i\ell \sin k_i\ell) +$$

$$+ (-\sin k_i\ell \cos k_i\ell + \text{sh}\, k_i\ell\, \text{ch}\, k_i\ell - 2\, \text{ch}\, k_i\ell \sin k_i\ell + 2\, \text{sh}\, k_i\ell \cos k_i\ell) +$$

$$+ 2\lambda_i(\sin^2 k_i\ell - 2\, \text{sh}\, k_i\ell \sin k_i\ell + \text{sh}^2 k_i\ell)] \tag{33}$$

Since the generalized force, Equation (30), is given in tabular form, then the solution of Equation (29) has to be obtained by numerical or graphical means.

I. Stringer Response

Due to continuity of the stringer at the frame, the ends of the stringers will be considered fixed. The transverse displacement of the stringers is much greater than that of the frame, and, for this reason, the motion of the fixed ends of the stringer will be neglected in obtaining

the stringer response. The dynamic displacement of the stringer is given by

$$\Phi(x, t) = \sum_i \phi_i(x)\, q_i(t)$$

where

$$\phi_i(x) = [\lambda_i(\cos k_i x - \text{ch}\, k_i x) + (\sin k_i x - \text{sh}\, k_i x)]$$

The generalized coordinates $q_i(t)$ satisfy the differential equation and the initial conditions given below

$$\ddot{q}_i(t) + \omega_i^2 q_i(t) = \frac{Q_i(t)}{M_i}\ , \quad q_i(0) = \dot{q}_i(0) = 0 \tag{34}$$

The $Q_i(t) = 7.74Eha\beta_i \left(\frac{q_{11}(t)}{b}\right)^3$, and the $\left(\frac{q_{11}(t)}{b}\right)^3$ is given in graphical form from the skin response in Figures 8, 9, and 10. Dimensional analysis shows that the time scales as b (i.e., $k_t = k_b$), and Figures 8, 9, and 10 can be used for the same a^4h/b^5 for the same peak pressure, P_o, and density, ρ, of the skin material. Equation (34) has to be integrated numerically or graphically.

In integrating Equation (34), a numerical procedure will be used and its formulation is established below. The $\ddot{q}_i(t)$ in terms of differences is given by

$$\ddot{q}_i(t_i) = \frac{q_i(t_i - 1) - 2q_i(t_i) + q_i(t_i + 1)}{(\Delta t)^2}$$

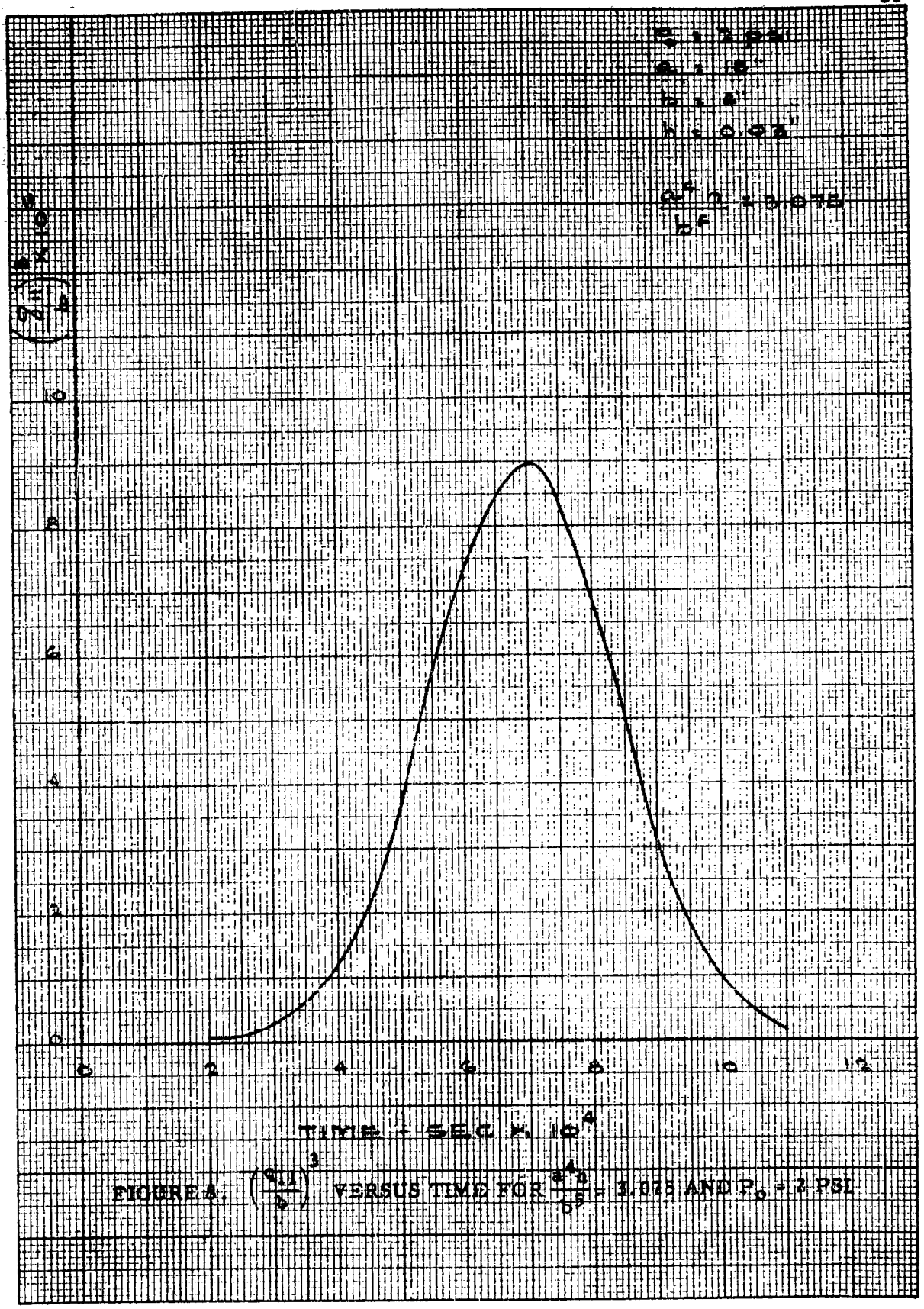

FIGURE A. $\left(\frac{qA}{b}\right)^3$ VERSUS TIME FOR $\frac{a^4\rho}{b^5}$ = 3.075 AND P_o = 2 PSI

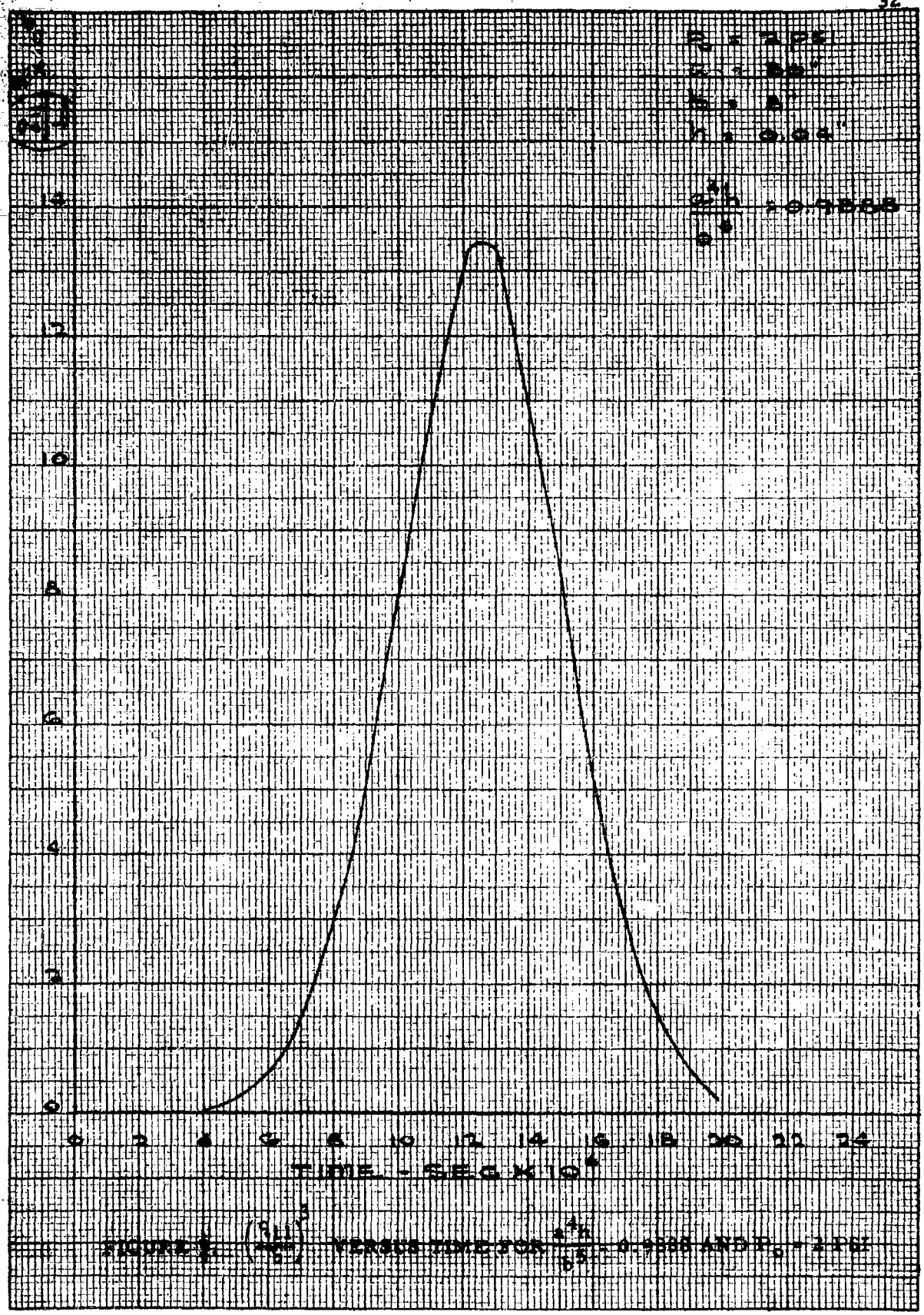

FIGURE 5. $\left(\frac{a_{11}}{a_{max}}\right)^3$ VERSUS TIME FOR $\frac{a^4 h}{b^5}$ = 0.9808 AND P_o = 2 PSI

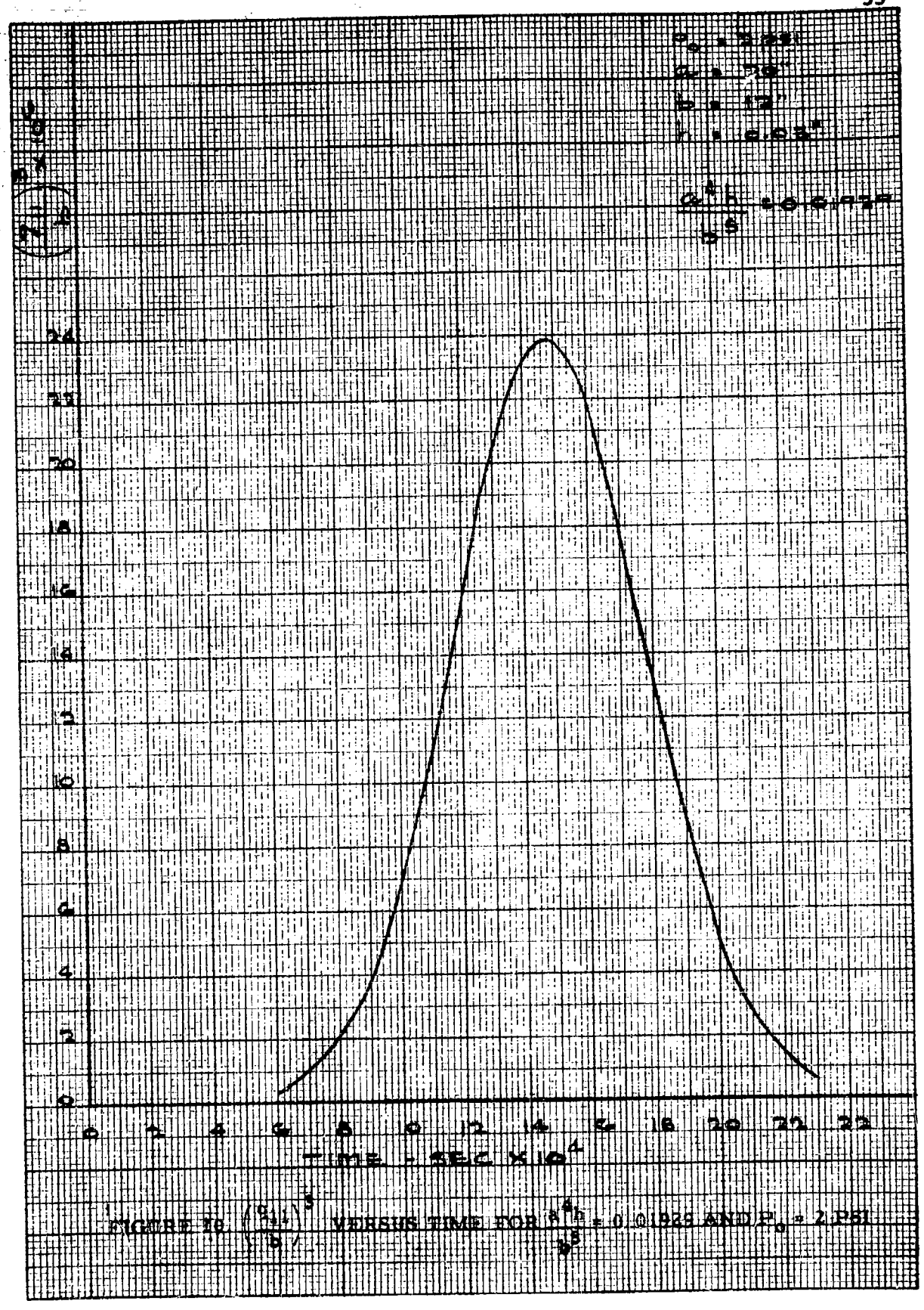

FIGURE 10. $\left(\frac{a}{b}\right)^3$ VERSUS TIME FOR $\frac{a^4 b}{D^5}$ = 0.01929 AND P_o = 2 PSI

then Equation (34) becomes

$$q_i(t_i - 1) - 2q_i(t_i) + q_i(t_i + 1) = - (\Delta t)^2 \omega_i^2 q_i(t_i) + \frac{Q_i(t_i)(\Delta t)^2}{M_i}$$

or

$$q_i(t_i + 1) = \frac{Q_i(t_i)(\Delta t)^2}{M_i} + [2 - (\Delta t)^2 \omega_i^2] q_i(t_i) - q_i(t_i - 1)$$

or

$$q_i(t_i + 1) = A_i(t_i) + B_i q_i(t_i) - q_i(t_i - 1) \qquad (35)$$

where

$$A_i(t_i) = \frac{7.74Eh}{m_i a \alpha_i} a\beta_i \left(\frac{q_{11}(t_i)}{b}\right)^3 (\Delta t)^2 = \frac{7.74Eh}{m_i \alpha_i} \beta_i \left(\frac{q_{11}(t_i)}{b}\right)^3 (\Delta t)^2$$

$$B_i = [2 - \omega_i^2 (\Delta t)^2]$$

ω_i = $(k_i^2)\sqrt{\frac{EI}{m_i}}$ = Frequency of the stringer

E = Modulus of elasticity of the stringer's material = 10.6×10^3 psi

h = Thickness of skin

m_i = Mass per unit length of stringer

a = Length of stringer

b = Width of panel

$q_{11}(t)$ = Generalized coordinate of the skin's response in the 1, 1th mode

(Δt) = Time interval

$k_1 a = 4.730;\ \alpha_1 = 1.244\ ;\ \beta_1 = 0.43682\ ;\ \lambda_1 = -1.0175$

$k_2 a = 7.853;\ \alpha_2 = 1.00088\ ;\ \beta_2 = 0.001212;\ \lambda_2 = -1.0008$

$k_3 a = 10.993;\ \alpha_3 = 1.000000;\ \beta_3 = -0.110407;\ \lambda_3 = -0.99997$

The moment on the stringer is given by

$$M = -EI\Phi''(x,t) = -EI\sum_i q_i(t)\phi_i''(x)$$

$$= -EI\sum_i q_i(t)\, k_i^2 [\lambda_i(-\cos k_i x - \text{ch}\, k_i x) + (-\sin k_i x - \text{sh}\, k_i x)]$$

The maximum moment was found to take place at x = 0 and thus

$$M_{max} = M|_{x=0} = -EI\sum_i q_i(t)\, k_i^2(-2\lambda_i) = 2EI\sum_i q_i(t)\, k_i^2 \lambda_i$$

$$\therefore M_{max} = \frac{2EI}{a^2}\sum_i q_i(t)(k_i a)^2 \lambda_i \qquad (36)$$

The shear is given by

$$V = -EI\Phi''' = -EI\sum_i q_i(t)\,\phi_i'''(x)$$

$$= -EI\sum_i q_i(t)\, k_i^3 [\lambda_i(\sin k_i x - \text{sh}\, k_i x) + (-\cos k_i x - \text{ch}\, k_i x)]$$

The stringer's reaction is equal to $V\big|_{x=0}$

$$V\Big|_{x=0} = -EI \sum_i q_i(t)\, k_i^3 (-2) = 2EI \sum_i q_i(t)\, k_i^3$$

$$\therefore \quad V\Big|_{x=0} = \frac{2EI}{a^3} \sum_i q_i(t)(k_i a)^3 \tag{37}$$

Stringer cross sections that are considered to be typical are shown in Figure 11. The (a) has been used in computing the stringer response using Equation (35). The effective mass per unit length of stringer is not easily determined because of the unknown interaction of the skin. For this reason, first, the response of the stringers was determined without any interaction of the skin (i.e., m_i = mass per unit length of the stringer), and the results are given in Figures 12 and 13. Also, computations were made with full interaction of the skin, as shown in Figure 14, which resulted in increasing the effective mass per unit length of stringer by a factor of about three. The response of the stringer was determined, and the obtained moments and stress were found about 30% smaller than without any skin interaction.

Because of the fact that an interaction of skin and stringer exists and is between complete and zero interaction, it is believed that such an interaction will reduce the response given in Figures 12 and 13 by 15%. Thus, if the values given in Figures 12 and 13 are modified by -15%, they are going to represent the true response of the stringer to within 5%, and this is considered satisfactory for the problem at hand. Such modified curves for direct use in design are given in Figures 15 and 16.

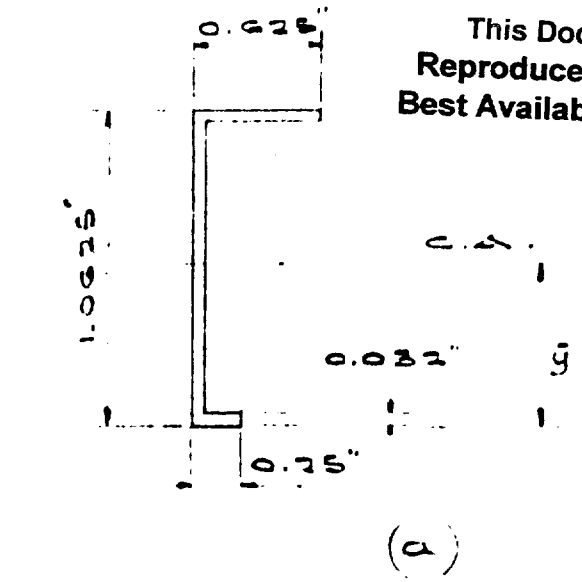

(a)

$\bar{y}$ = 0.614 in.

I = 0.00950 $in.^4$

A = 0.060 in^2

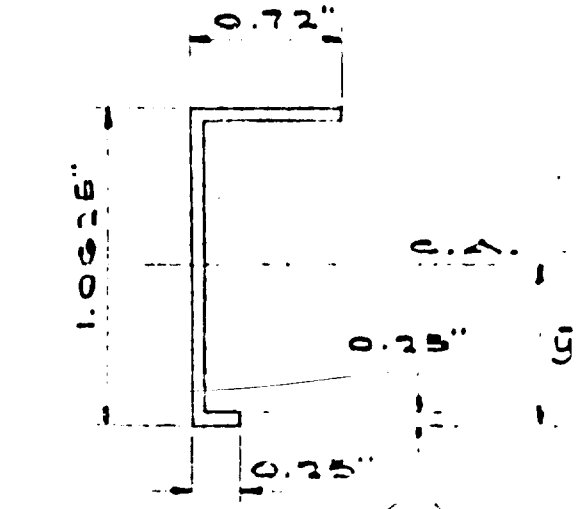

(b)

$\bar{y}$ = 0.6542 in.

I = 0.007941 in^4

A = 0.04956 in^2

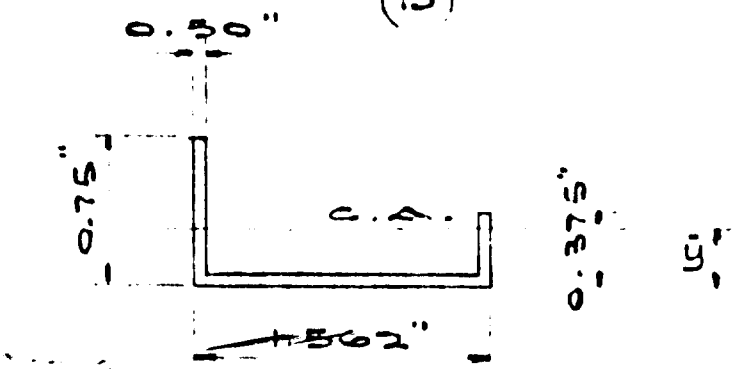

(c)

$\bar{y}$ = 0.14996 in.

I = 0.0049261 in^4

A = 0.12935 in^2

FIGURE 11. TYPICAL CROSS SECTIONS OF STRINGERS

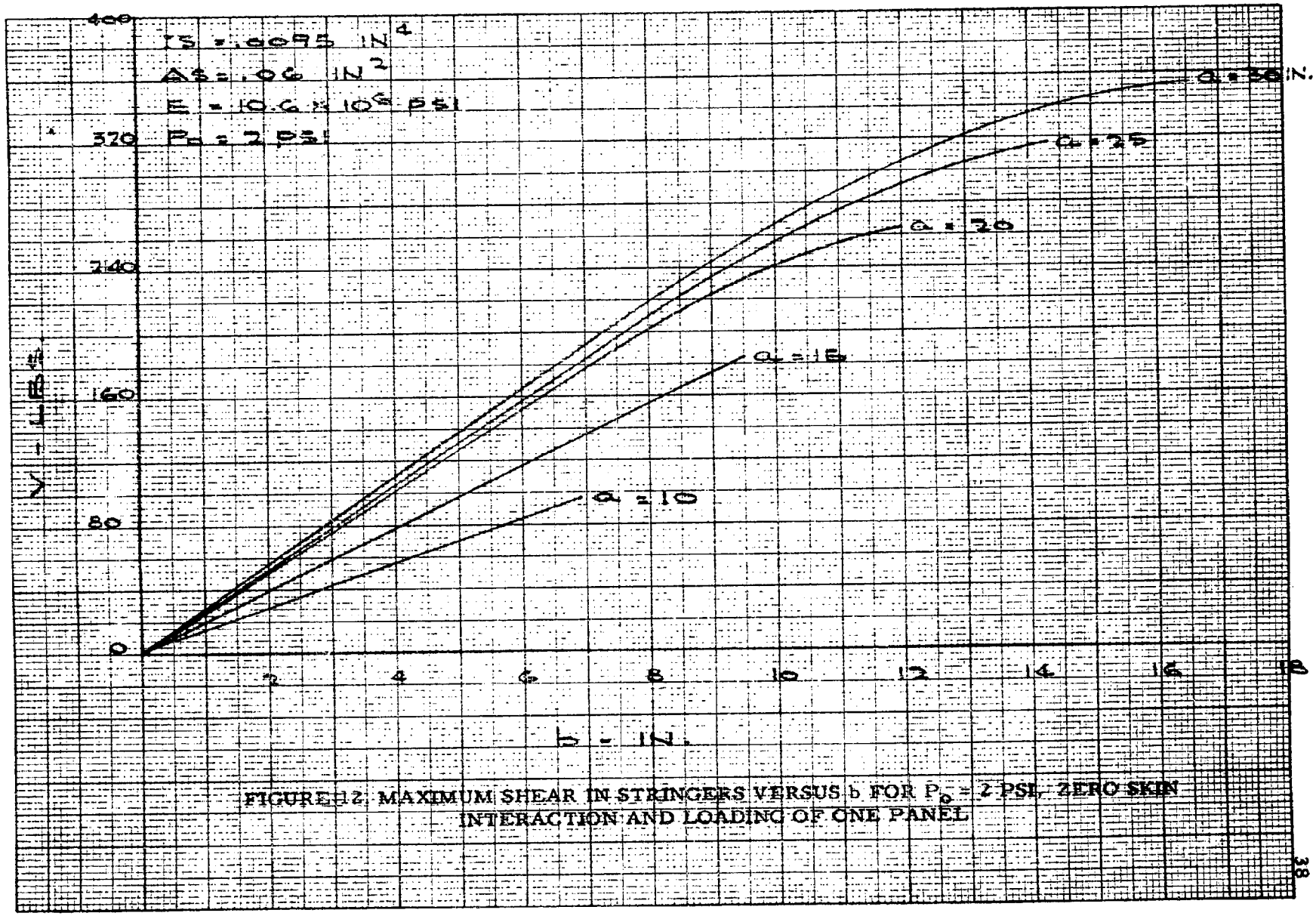

FIGURE 12. MAXIMUM SHEAR IN STRINGERS VERSUS b FOR P_o = 2 PSI, ZERO SKIN INTERACTION AND LOADING OF ONE PANEL

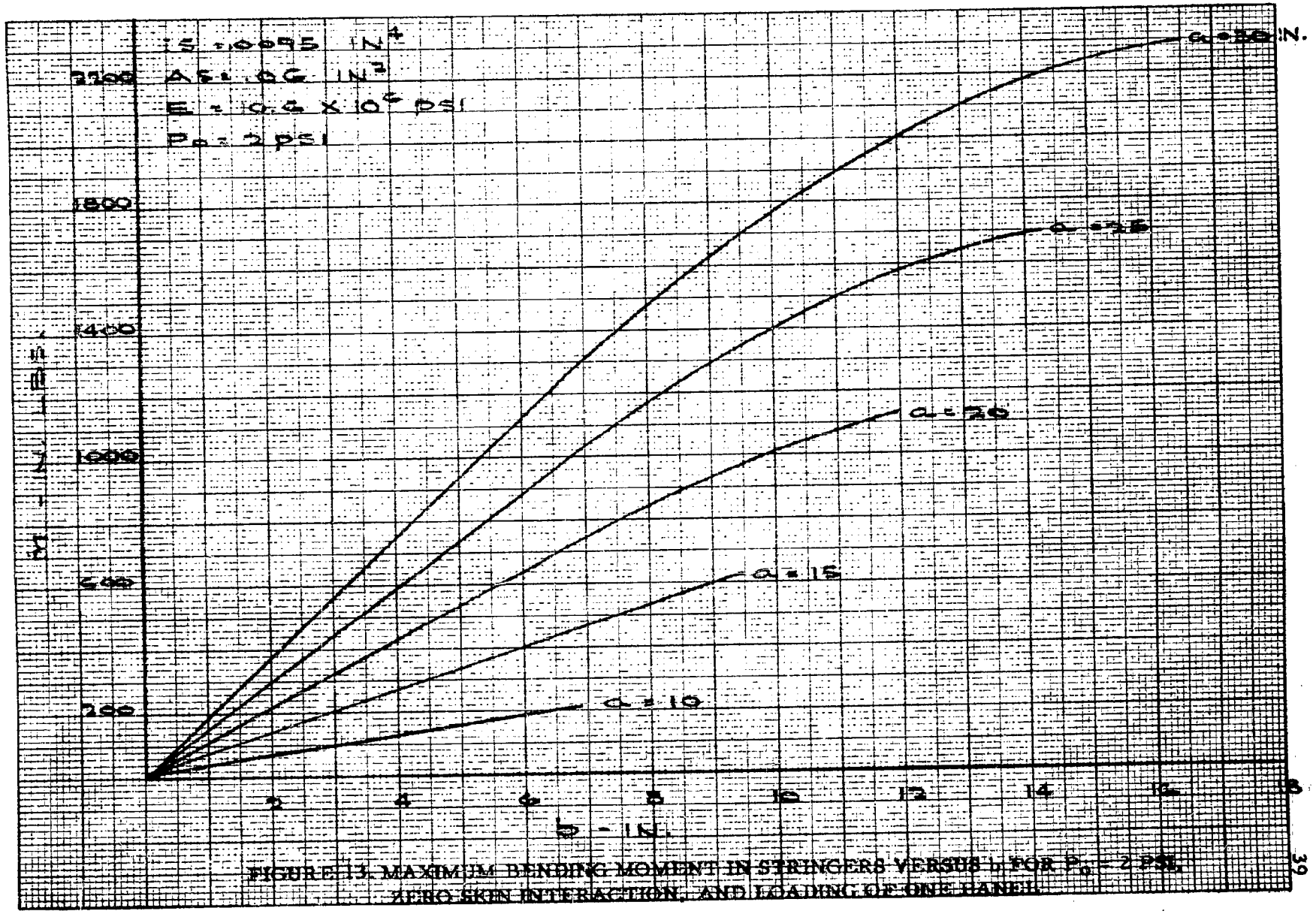

FIGURE 13. MAXIMUM BENDING MOMENT IN STRINGERS VERSUS b FOR $P_0 = 2$ PSI, ZERO SKIN INTERACTION, AND LOADING OF ONE PANEL

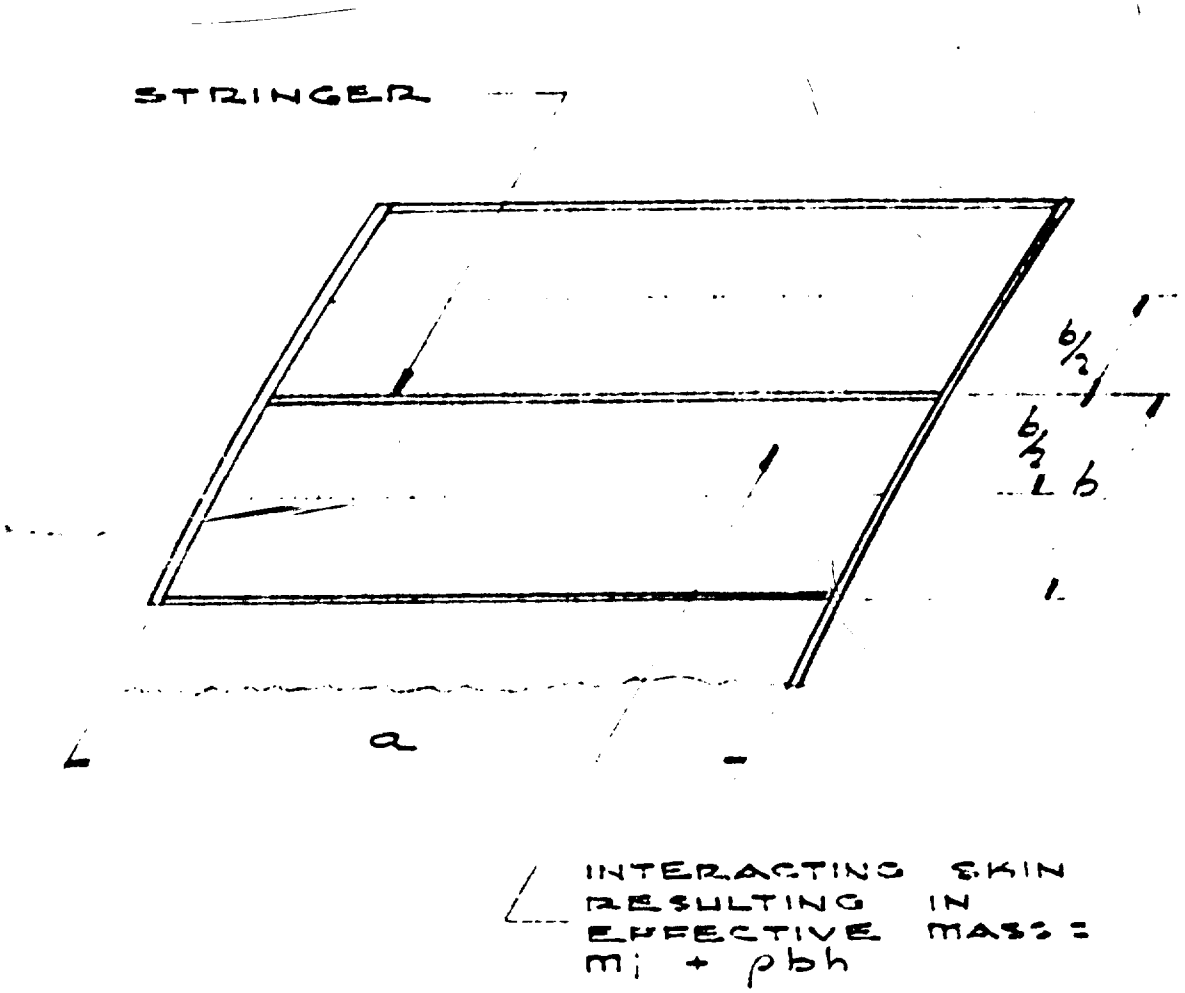

FIGURE 14. SCHEMATIC REPRESENTATION OF FULL SKIN INTERACTION

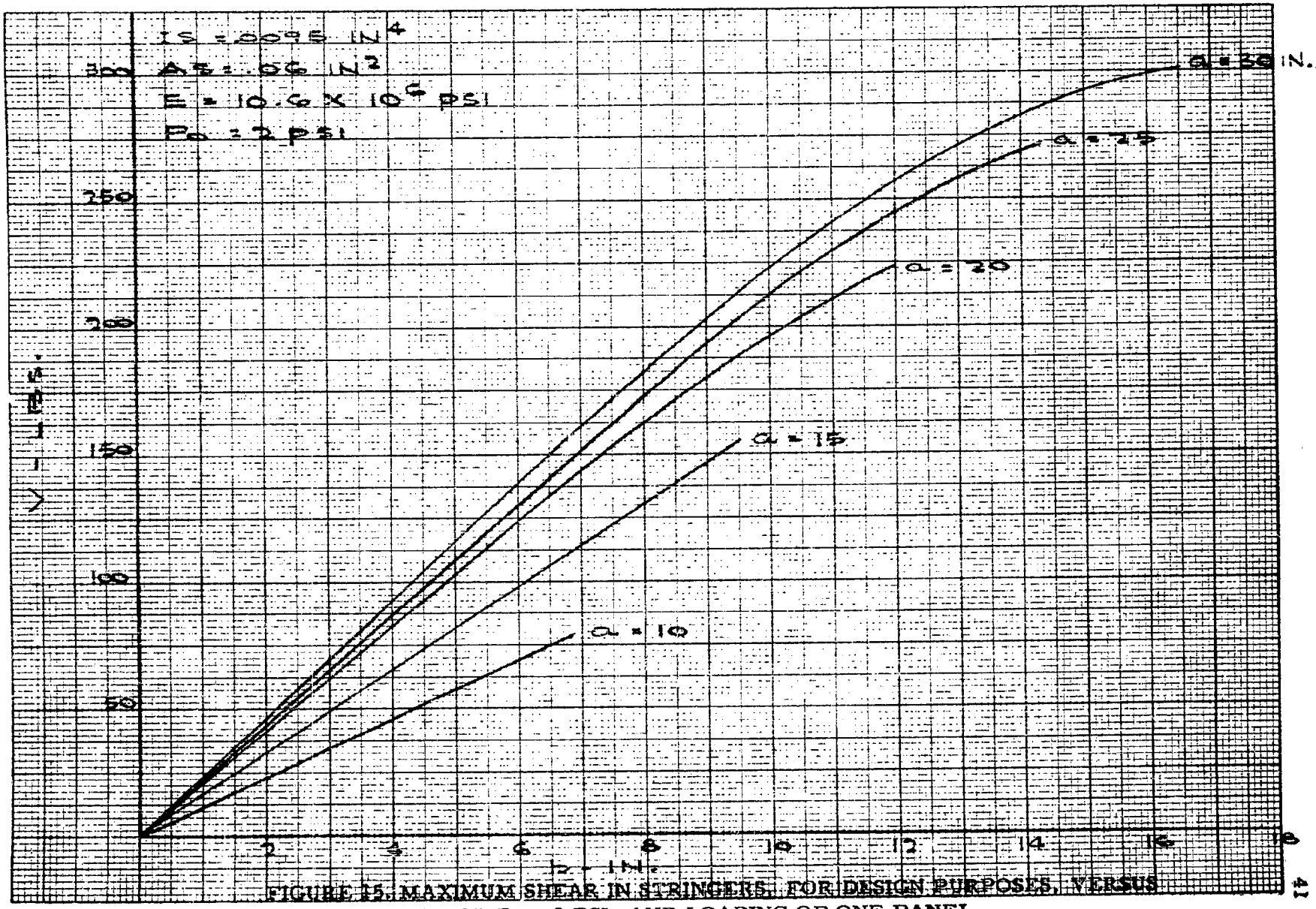

FIGURE 15. MAXIMUM SHEAR IN STRINGERS, FOR DESIGN PURPOSES, VERSUS b FOR P_o = 2 PSI, AND LOADING OF ONE PANEL

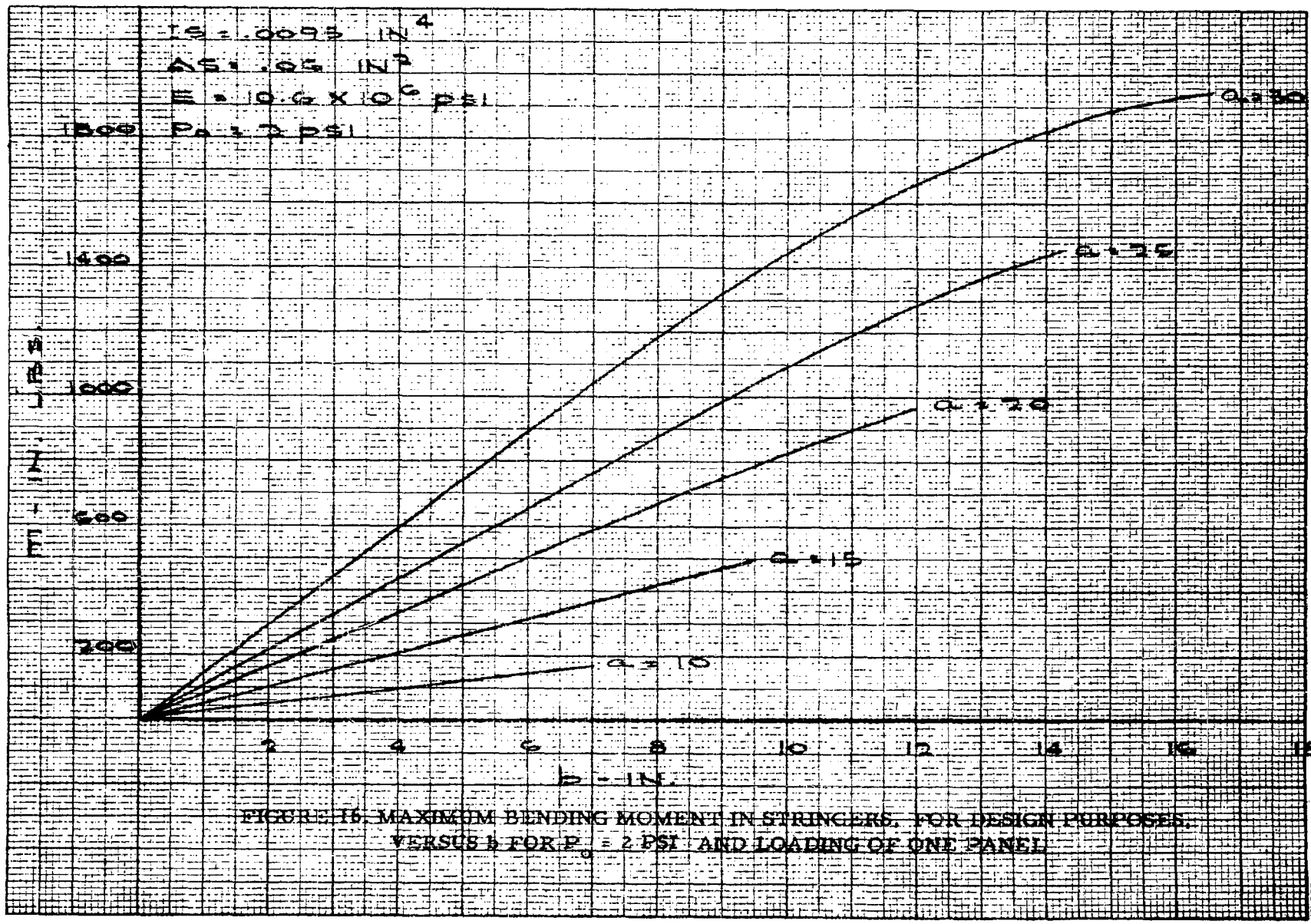

FIGURE 16. MAXIMUM BENDING MOMENT IN STRINGERS, FOR DESIGN PURPOSES, VERSUS b FOR P_o = 2 PSI AND LOADING OF ONE PANEL

Loading curves as well as modified curves for direct use in design have been obtained for peak pressure intensity P_o = 1 psi and are given in Figures 17 through 21.

Based on the discussion that follows, the results presented in Figures 15, 16, 20, and 21 can be used for other stiffeners as well.

For a stringer with the same I/m_i as the one used herein, the frequency will be the same, and, for an increase of m_i by 50% and even 100%, the moment and shear will be proportional to I and not off by more than -10%. The bending stresses are the critical ones in a stringer; thus, for the same I/m_i as the one used herein and an increase of m_i by 50% or 100%, the bending moments will be proportional to I and not off by more than -10%. In this way, the results of Figures 15, 16, 20, and 21 can be used for design purposes when determination of maximum stress in the stringer with less than ±10% off can be tolerated.

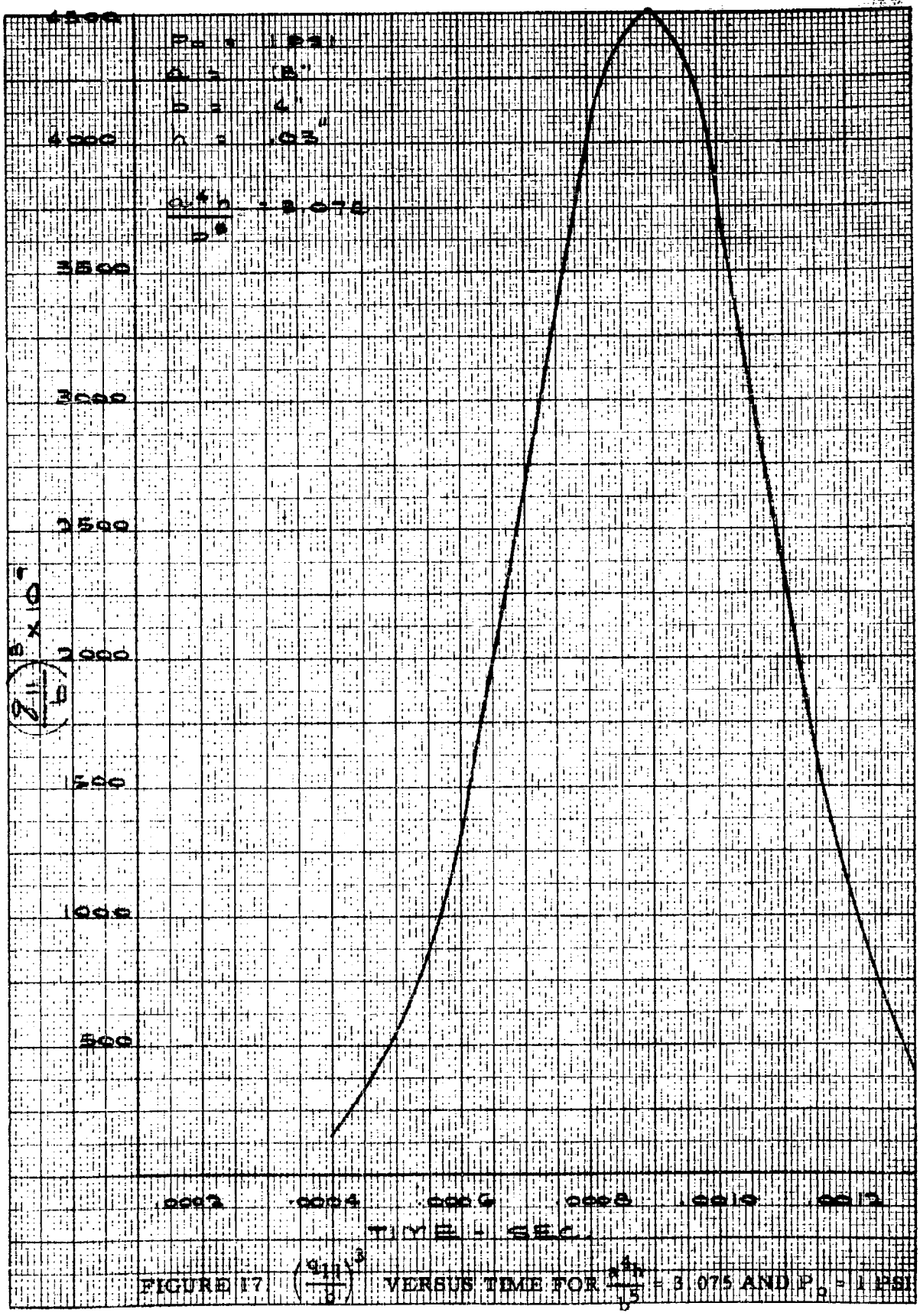

FIGURE 17 $\left(\frac{q_{11}}{g}\right)^3$ VERSUS TIME FOR $\frac{a^4 h}{b^5}$ = 3.075 AND P_o = 1 PSI

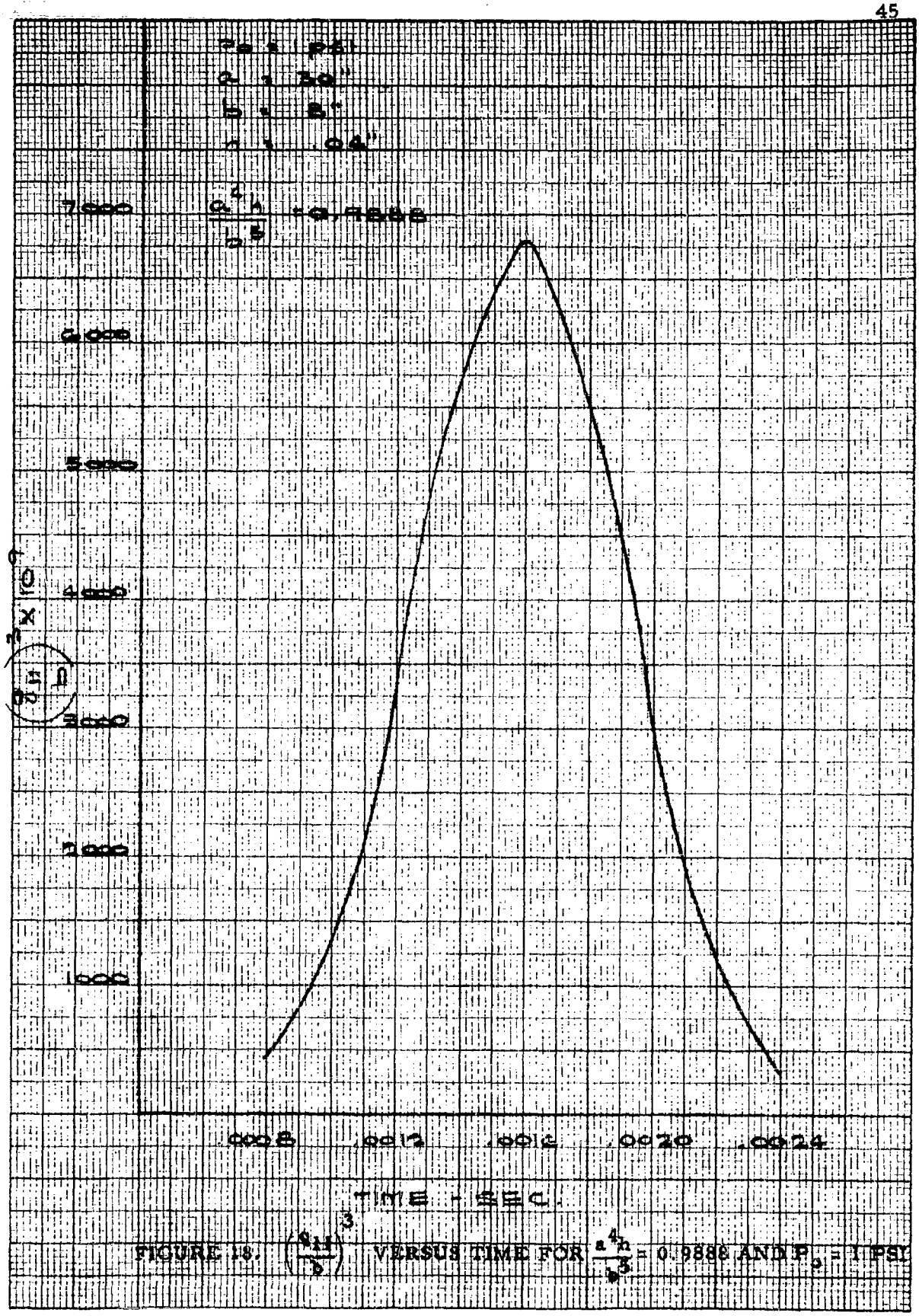

FIGURE 18. $\left(\frac{q_{11}}{b}\right)^3$ VERSUS TIME FOR $\frac{a^4 h}{b^3}$ = 0.9888 AND P_o = 1 PSI

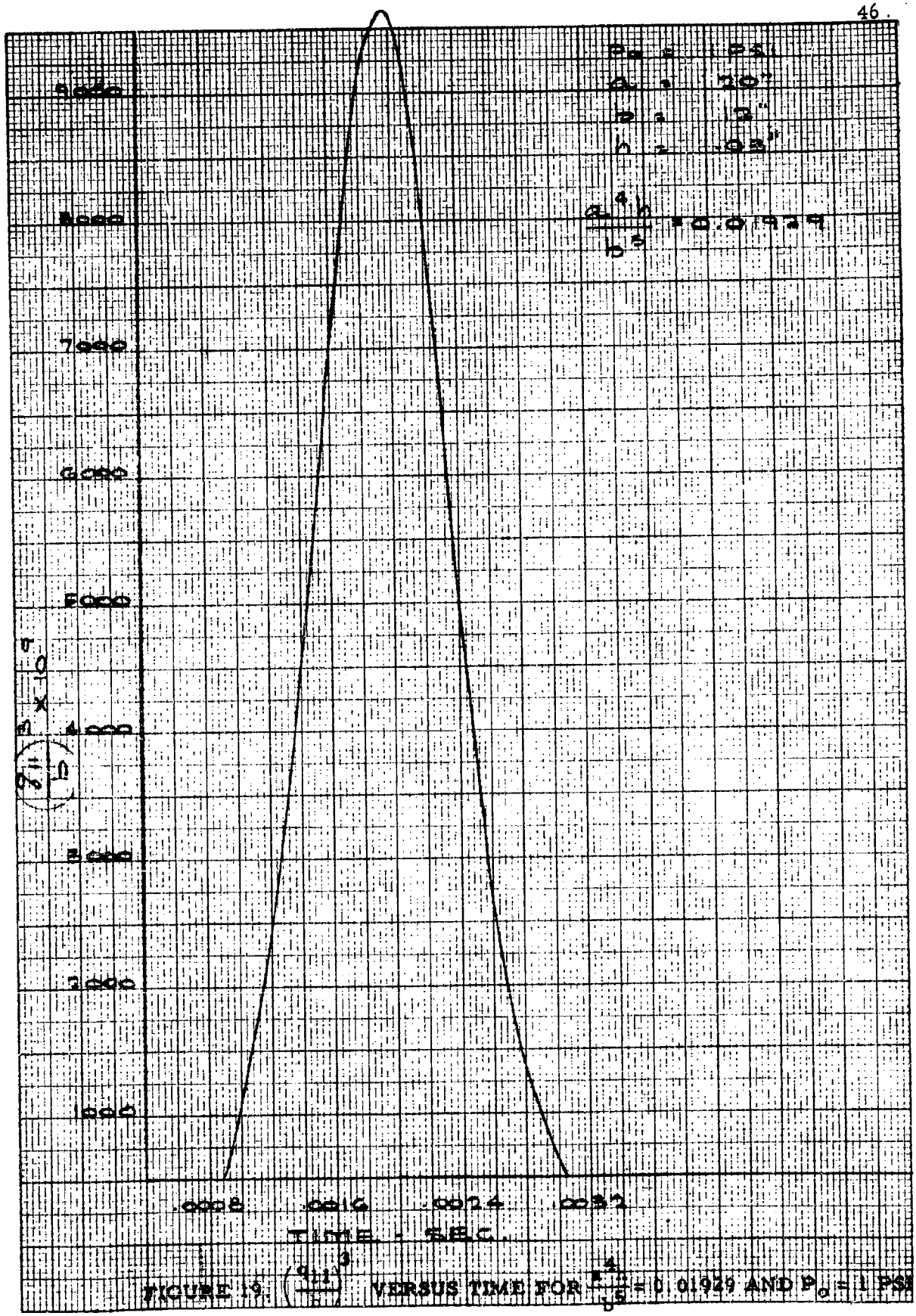

FIGURE 19. $\left(\frac{q_{11}}{h}\right)^3$ VERSUS TIME FOR $\frac{A}{b^5}$ = 0.01929 AND P_o = 1 PSI

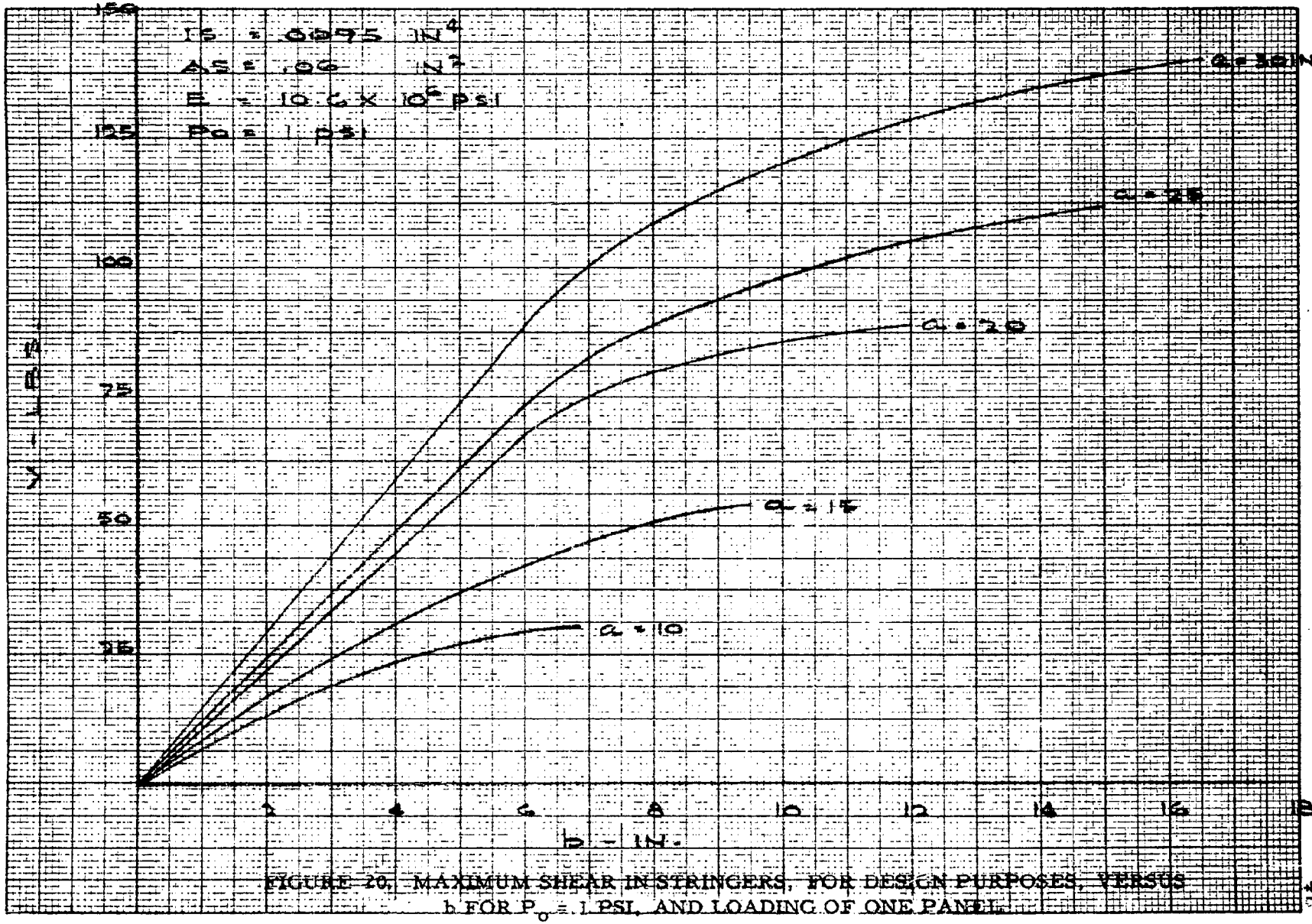

FIGURE 20. MAXIMUM SHEAR IN STRINGERS, FOR DESIGN PURPOSES, VERSUS b FOR P_o = 1 PSI, AND LOADING OF ONE PANEL.

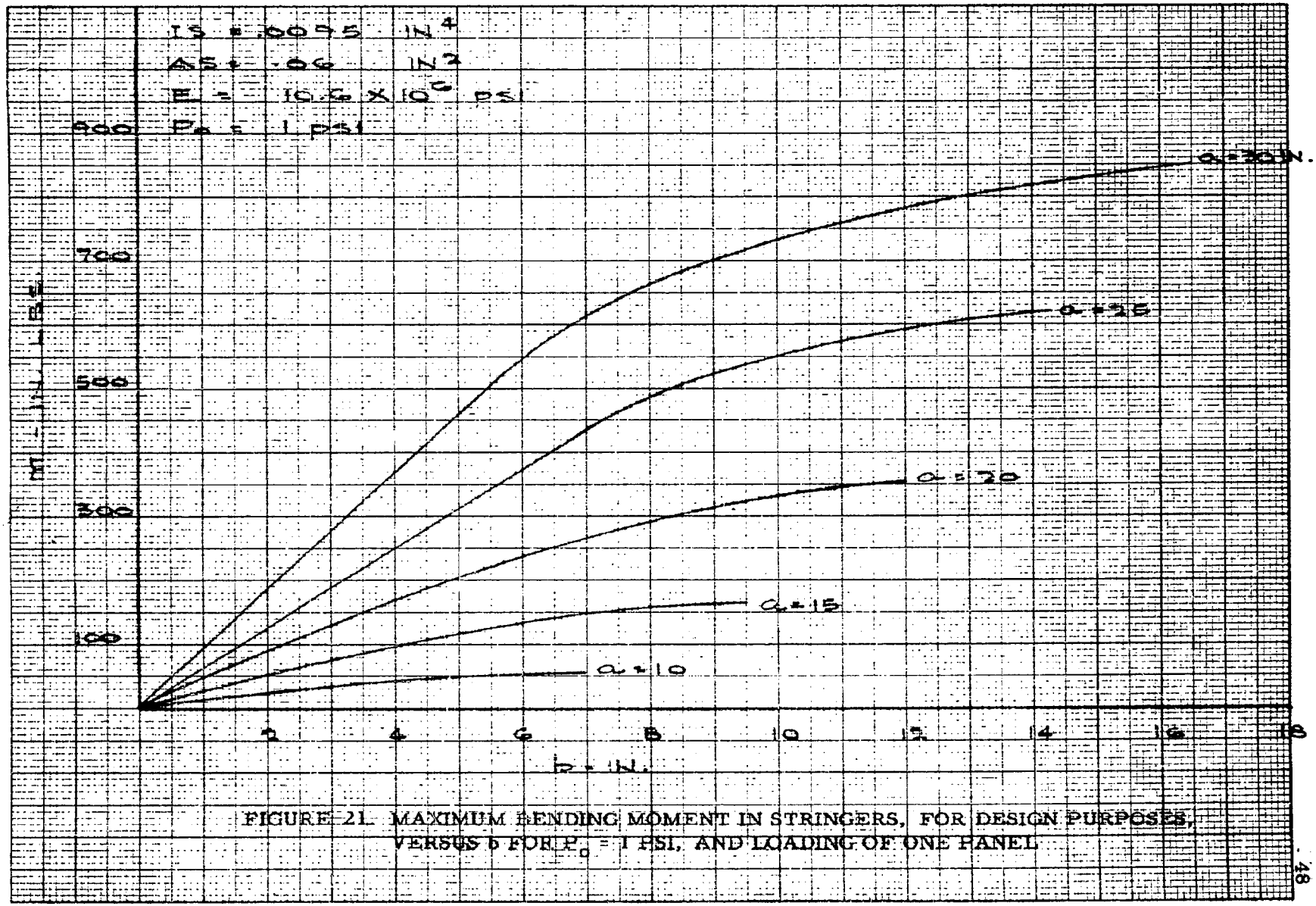

FIGURE 21. MAXIMUM BENDING MOMENT IN STRINGERS, FOR DESIGN PURPOSES, VERSUS b FOR P_o = 1 PSI, AND LOADING OF ONE PANEL

J. Formulation of the Approximate Flexural Dynamic Response of an Elliptical Ring

The differential equations of motion of an elliptical ring of constant cross section are linear of the fourth order with highly complex variable coefficients. Their solution in terms of known functions is inordinately difficult and is considered to be beyond the scope of this investigation. Thus, the true modes of vibration have not been determined.

Because of that, an approximate solution is sought on the basis of an assumed mode of fundamental vibration. A typical elliptical frame of a fuselage has been provided and is given in Figure 22. It is true that the cross section of the frame is not constant, and also that about seventy-five percent of its length has a constant cross section. Also, the frame under periodic loading along the circumference will deflect more in the direction of the minor axis than in the direction of the major axis of the ellipse. This difference in the magnitude of the above mentioned displacements becomes greater for greater ellipticities. The increase in rigidity at the ends of the major axis will result in a decrease of the displacements in that portion of the frame, and, at the same time, will decrease, in a smaller degree, the displacements of the frame where the cross section remains constant. It is believed that the ratio of the areas under the static deflection curve for a frame with constant cross section and the same ratio of the areas under the deflection curve for a frame with increased rigidity at the ends of the major axis, under the same loading, and whose

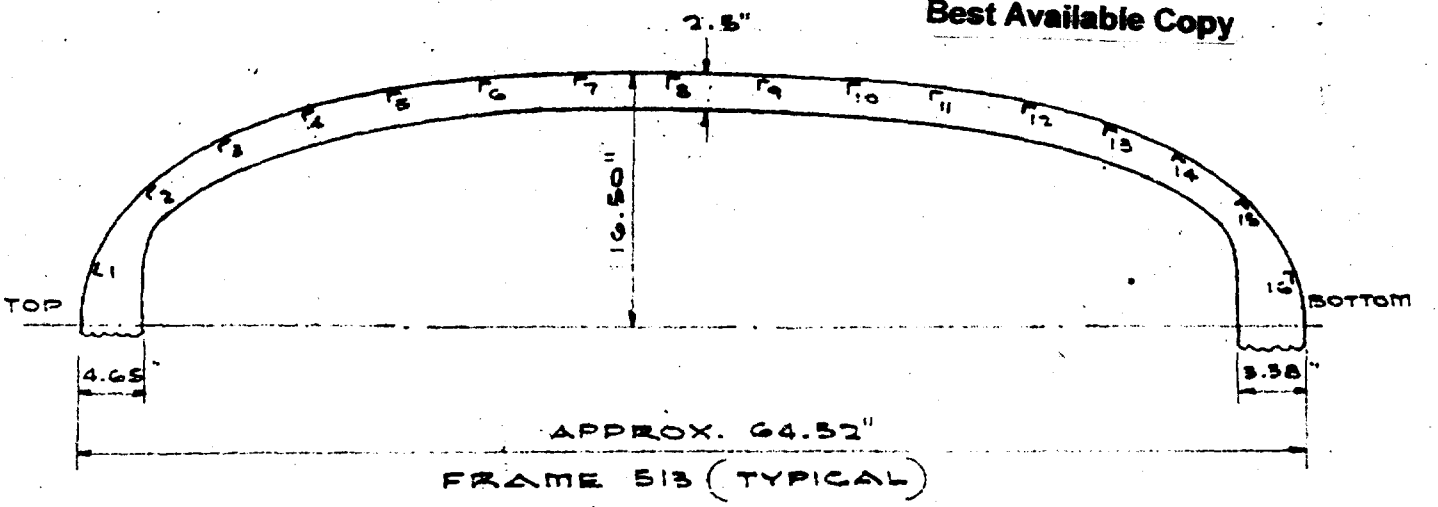

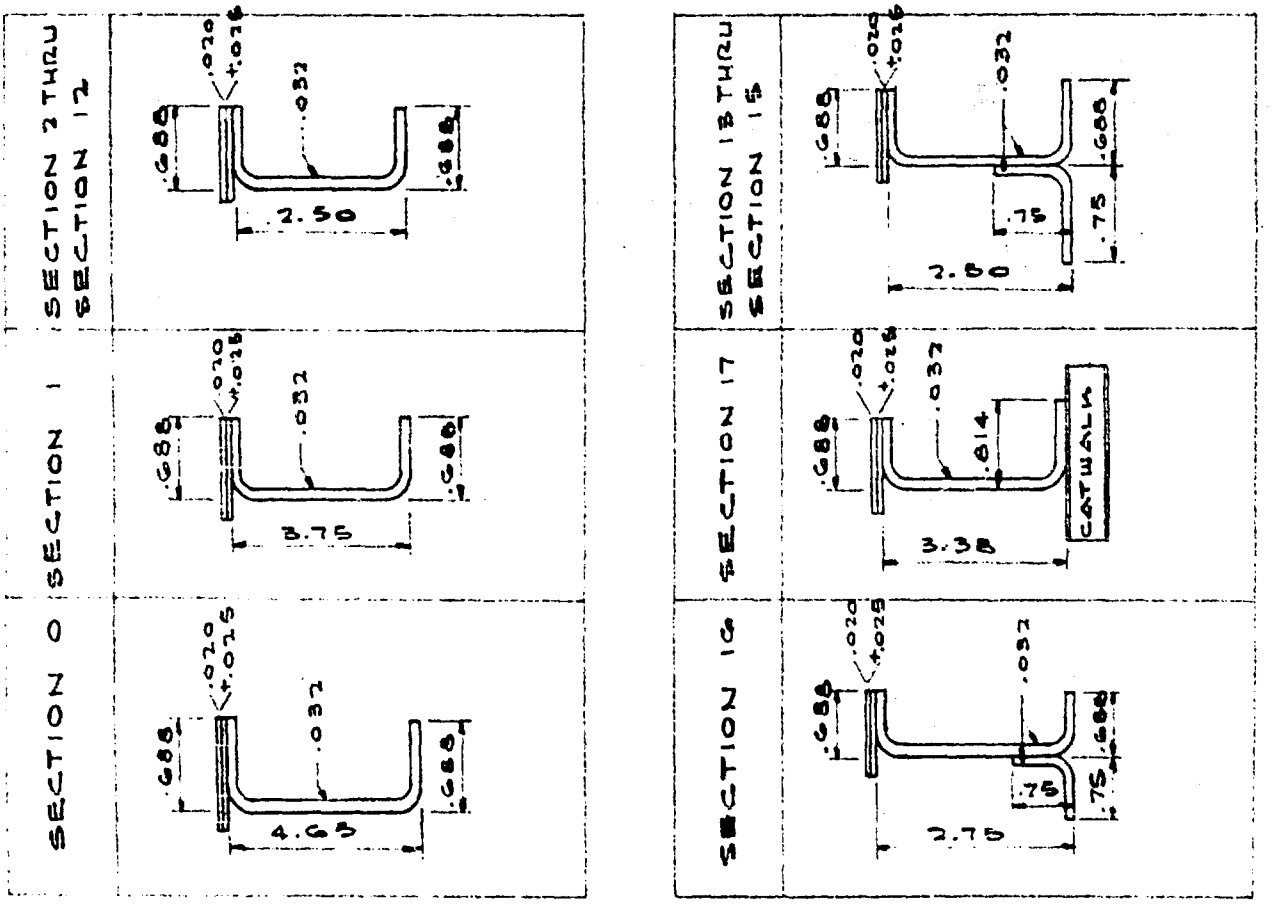

FIGURE 22. TYPICAL FRAME

seventy-five percent of the length has a constant cross section, differ but little. If the dynamic response of the constant section and variable section frame is considered on the basis of their static deflection curve mode, the generalized force (i.e., load times mode displacement) for both frames will be essentially the same for both frames. If the generalized mass is considered (i.e., mass times mode displacement squared) it will differ very little for the two frames, because the increase in mass takes place only on twenty-five percent of the frame length, and because the displacement in that portion of the frame is much smaller than in the flat portion of the ellipse. In addition, the frequency of the constant section and variable section frames will be different by a small amount which will cause only a slight shift in the time of maximum response, leaving the magnitude of the generalized displacement slightly affected. Based on the above discussion, it is believed that under the loading at hand the frame with localized increase in rigidity and one with constant cross section, equal to the one existing on the seventy-five percent of the frame with variable cross section, will have practically the same deflected shape and dynamic response.

It is known that any deflection curve can be expressed in terms of the natural modes. In the absence of the true modes, it is believed that the best approximate shape to be used as a mode would be the static deflection curve.

The loading of the frame is concentrated, coming from the stringers' reactions, and distributed, coming from the skin. Due to relatively close spacing of the stringers, the static deflection curve under this loading will be close to the static deflection curve of the constant section elliptical ring under uniform loading. Such a deflection curve is not difficult to obtain, and for an approximate treatment it is considered satisfactory.

As a result of the above reasoning, the approximate flexural dynamic response of the elliptical ring at hand will be based on the static deflection curve mode under uniform loading. Such a mode is shown in Figure 23.

If it is denoted by $\phi(s)$, where s is the measure of length of the ellipse, then the dynamic displacement is given by

$$\Phi(s,t) = \phi(s)\, q(t) \tag{38}$$

where the $q(t)$ satisfies the differential equation and initial conditions

$$\ddot{q}(t) + \omega^2 q(t) = \frac{Q(t)}{M} \quad ; \quad q(0) = \dot{q}(0) = 0 \tag{39}$$

where ω = the frequency and is given by

$$\omega^2 = \frac{EI \int_0^{\pi/2} \left[\frac{\partial^2 \phi(s)}{\partial s^2}\right]^2 ds}{m_i \int_0^{\pi/2} \phi^2(s)\, ds} \quad ; \quad \left[0 \text{ to } \pi/2 \text{ due to symmetry of } \phi(s)\right] \tag{40}$$

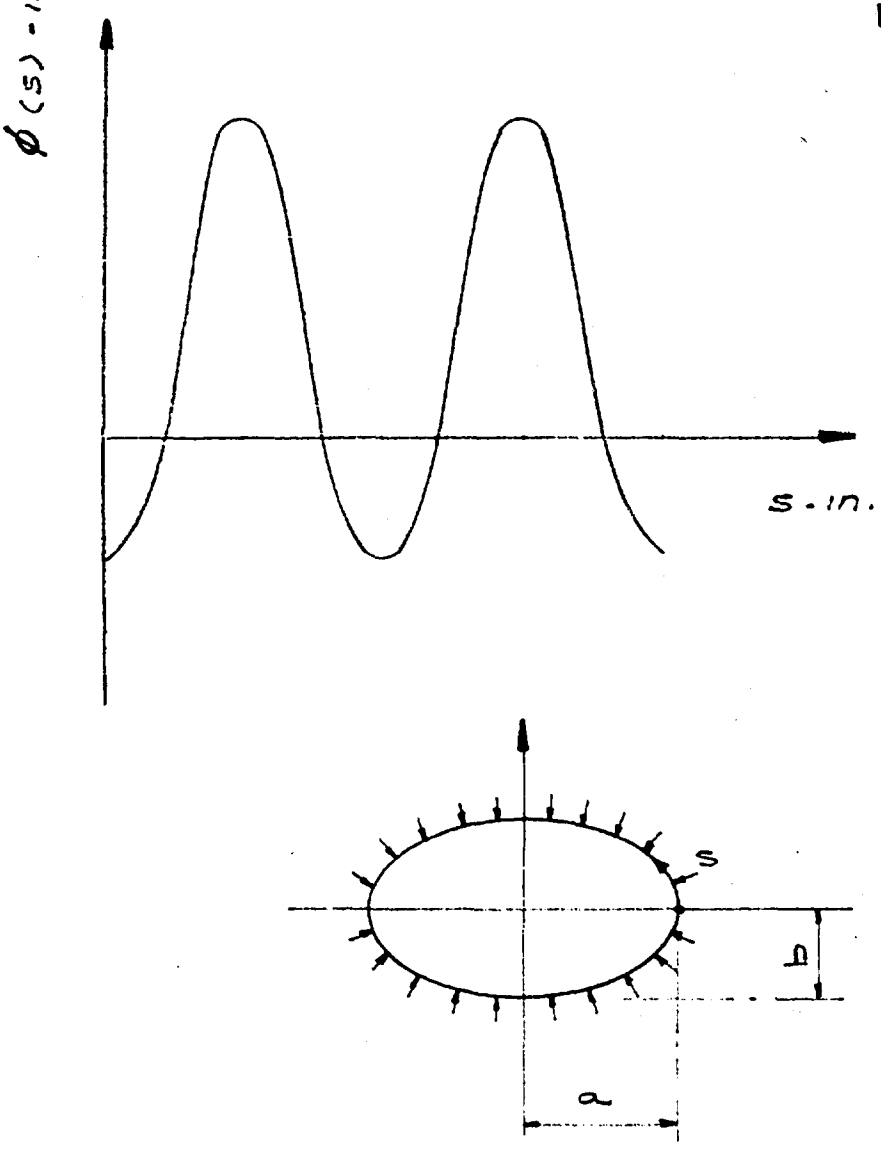

FIGURE 23.
STATIC DEFLECTION CURVE
OF ELLIPTICAL RING UNDER UNIFORM PRESSURE

The $Q(t)$ = generalized force and is given by

$$Q(t) = Q_{sk}(t) + Q_{str}(t)$$

where $Q_{sk}(t)$ is the part of the generalized force coming from the skin loading of the frame, and, using Equation (24) for m = n = 1, the $Q_{sk}(t)$ is given by

$$Q_{sk}(t) = \sum_i 7.74Eh\left(\frac{q_{11}}{a}\right)^3 \int_{s=a_{1i}}^{s=a_{2i}} \sin^3\frac{\pi s}{b}\,\phi(s)\,ds$$

where a_{1i} and a_{2i} are the beginning and end of the ith panel. The $\left(\frac{q_{11}}{a}\right)^3$ are given for different values of $\frac{b^4h}{a^5}$ for P_o = 2 psi and P_o = 1 psi in Figures 24 through 29, and can be used as the $\left(\frac{q_{11}}{b}\right)^3$ curves were used for the stringer response.

The $Q_{str}(t)$ comes from the stringers' reactions, and, using Equation (37) with only the first mode, which is sufficient in this problem as is shown in sample calculations, the $Q_{str}(t)$ is given by

$$Q_{str}(t) = \sum_i 2V\Big|_{x=0} = \sum_i \frac{4EI}{a^3}\,q_1(t)(k_1a)^3\,\phi(a_{1i})$$

Then

$$Q_{str}(t) = \sum_i 7.74Eh\left(\frac{q_{11}}{a}\right)^3 \int_{s=a_{1i}}^{s=a_{2i}} \sin^3\frac{\pi s}{b}\,\phi(s)\,ds + \sum_i \frac{4EI}{a^3}\,q_1(t)(k_1a)^3\,\phi(a_{1i}) \qquad (41)$$

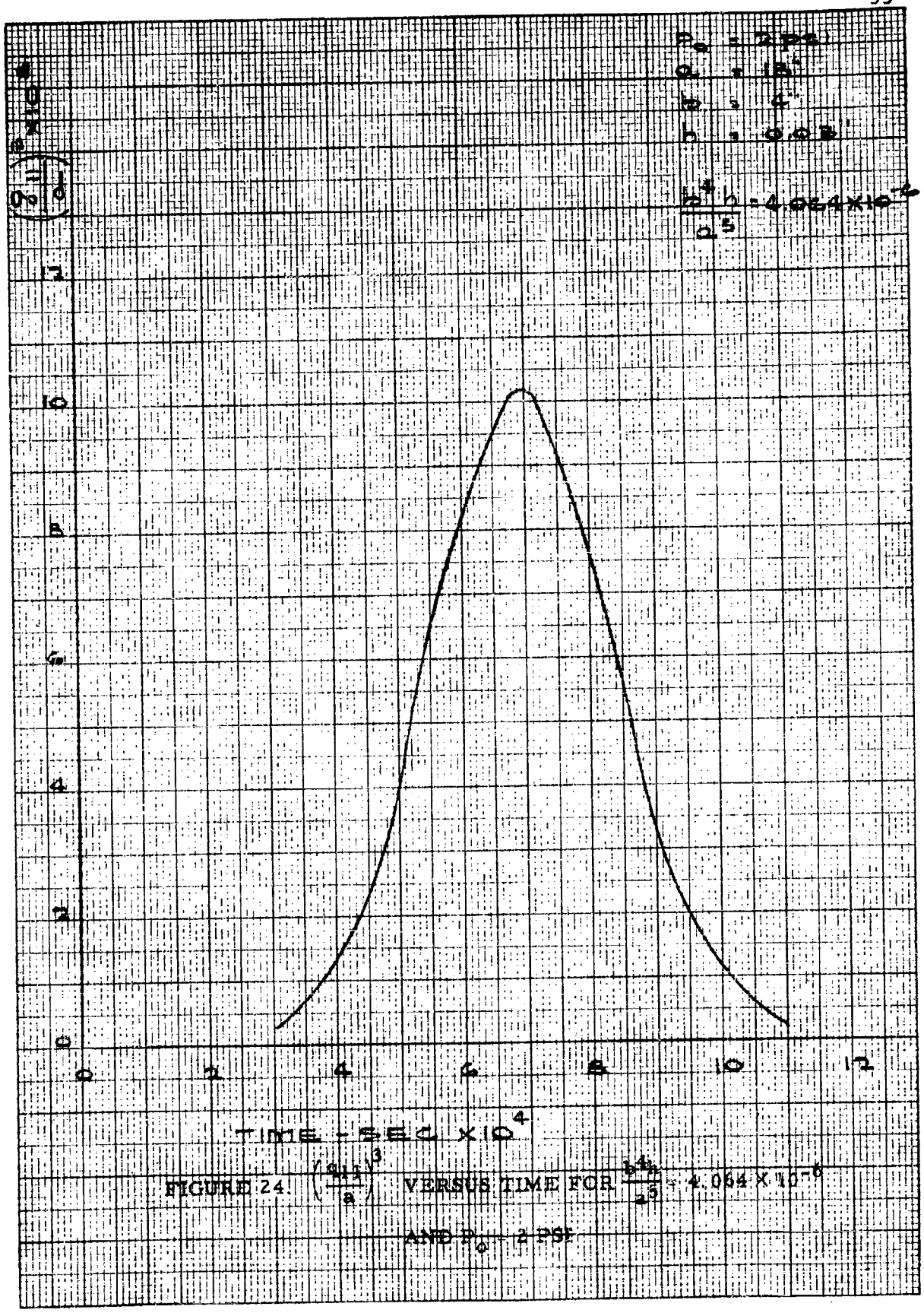

FIGURE 24. $\left(\frac{a_{max}}{a}\right)^3$ VERSUS TIME FOR $\frac{b^4 h}{a^5} = 4.064 \times 10^{-6}$ AND $P_0 = 2$ PSI

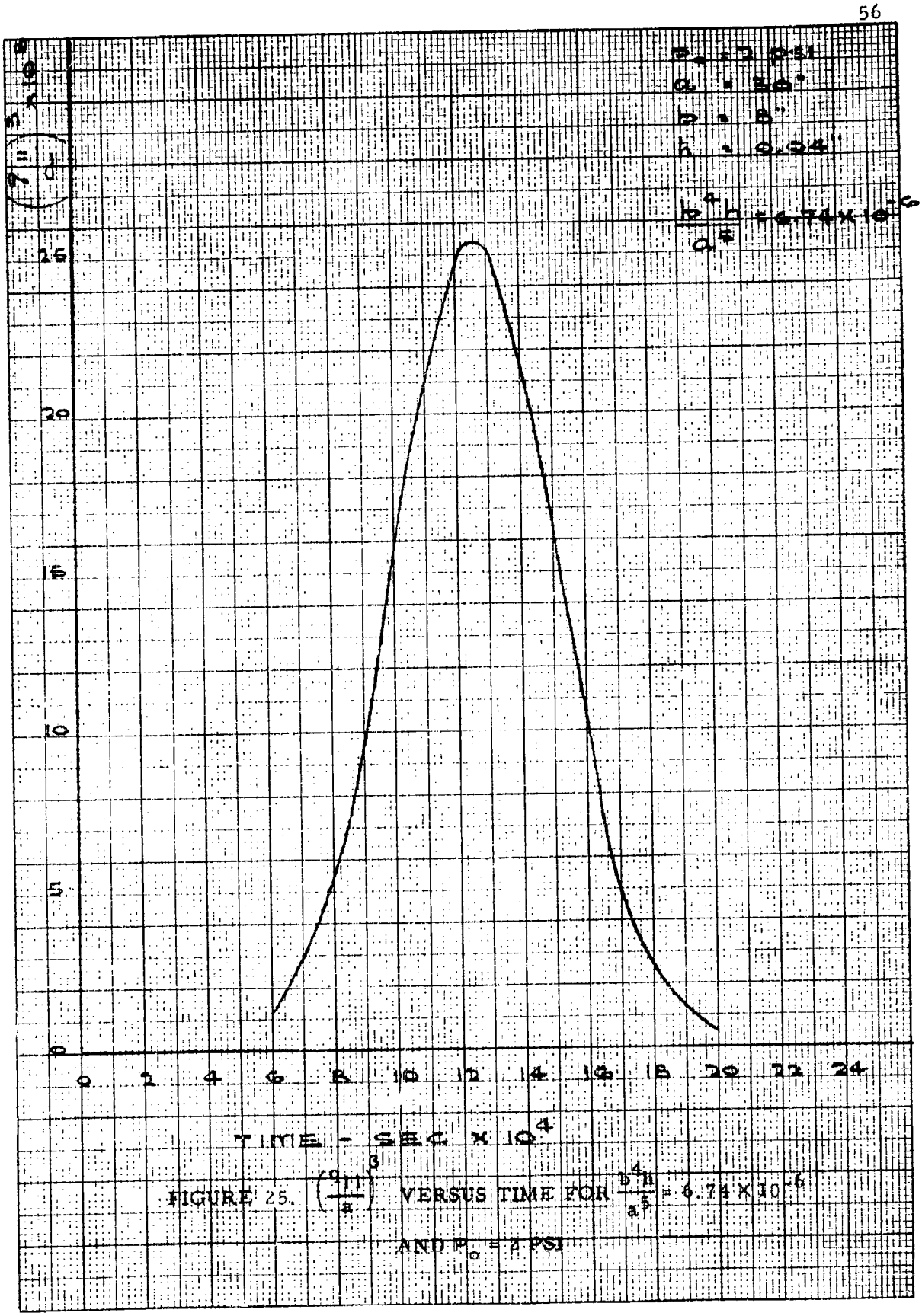

FIGURE 25. $\left(\frac{q_{11}t}{a}\right)^3$ VERSUS TIME FOR $\frac{b^4h}{a^5}$ = 6.74 X 10⁻⁶ AND P_o = 2 PSI

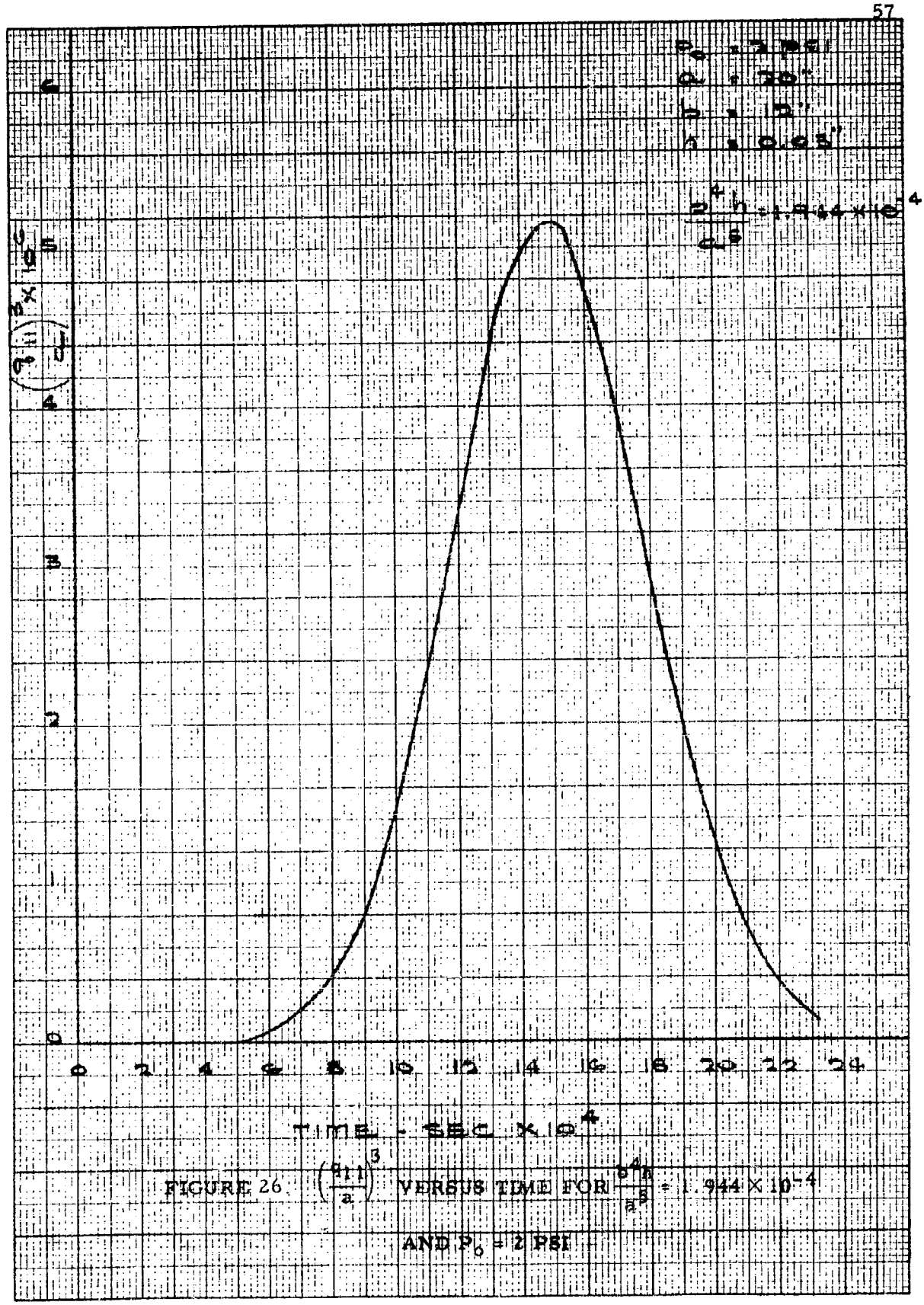

FIGURE 26 $\left(\frac{q_{1,1}}{a}\right)^3$ VERSUS TIME FOR $\frac{b^4 h}{a^5} = 1.944 \times 10^{-4}$ AND $P_o = 2$ PSI

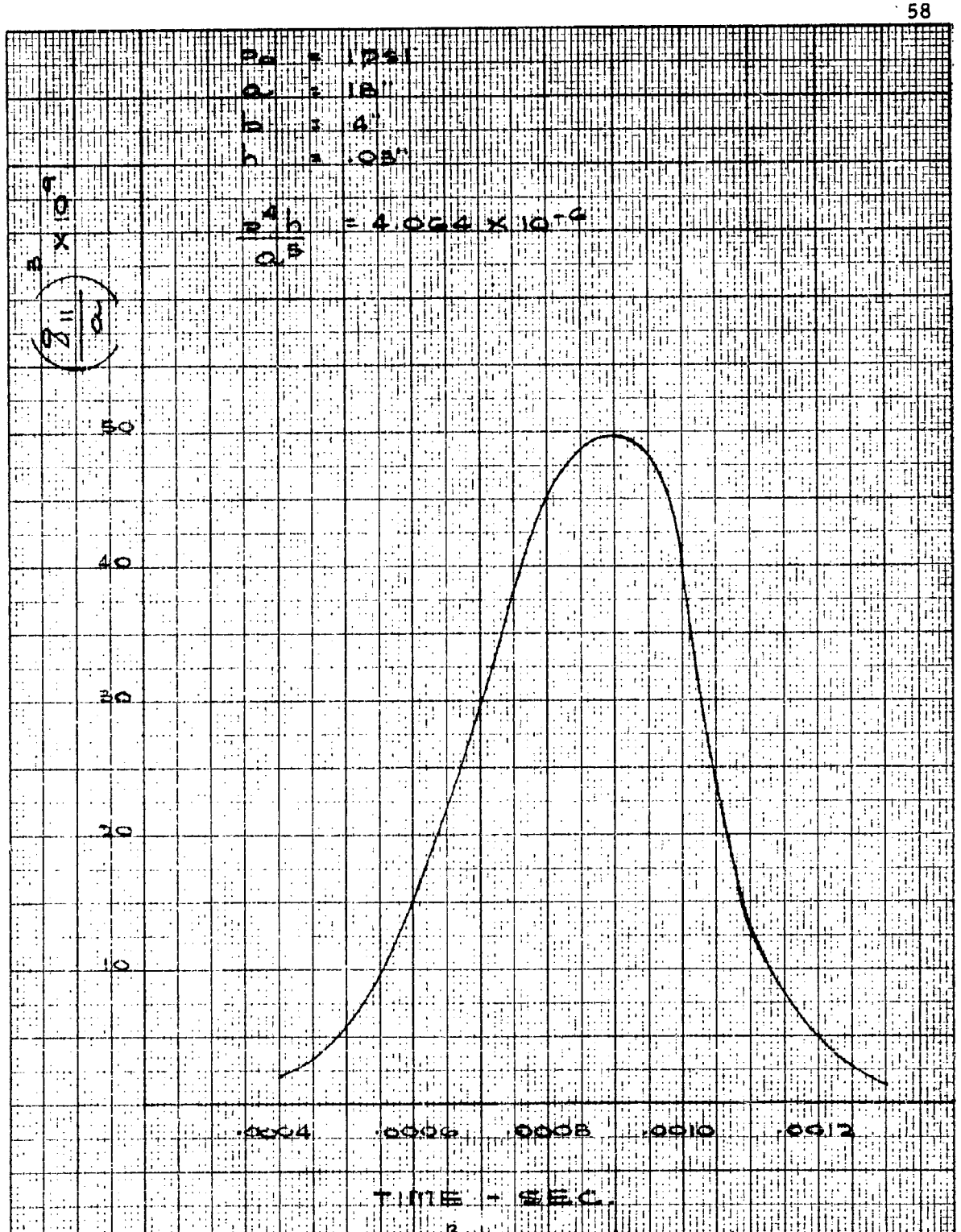

FIGURE 27. $\left(\frac{q_{11}}{a}\right)^3$ VERSUS TIME FOR $\frac{b^4 h}{a^5}$ = 4.064 × 10⁻⁶ AND P_o = 1 PSI

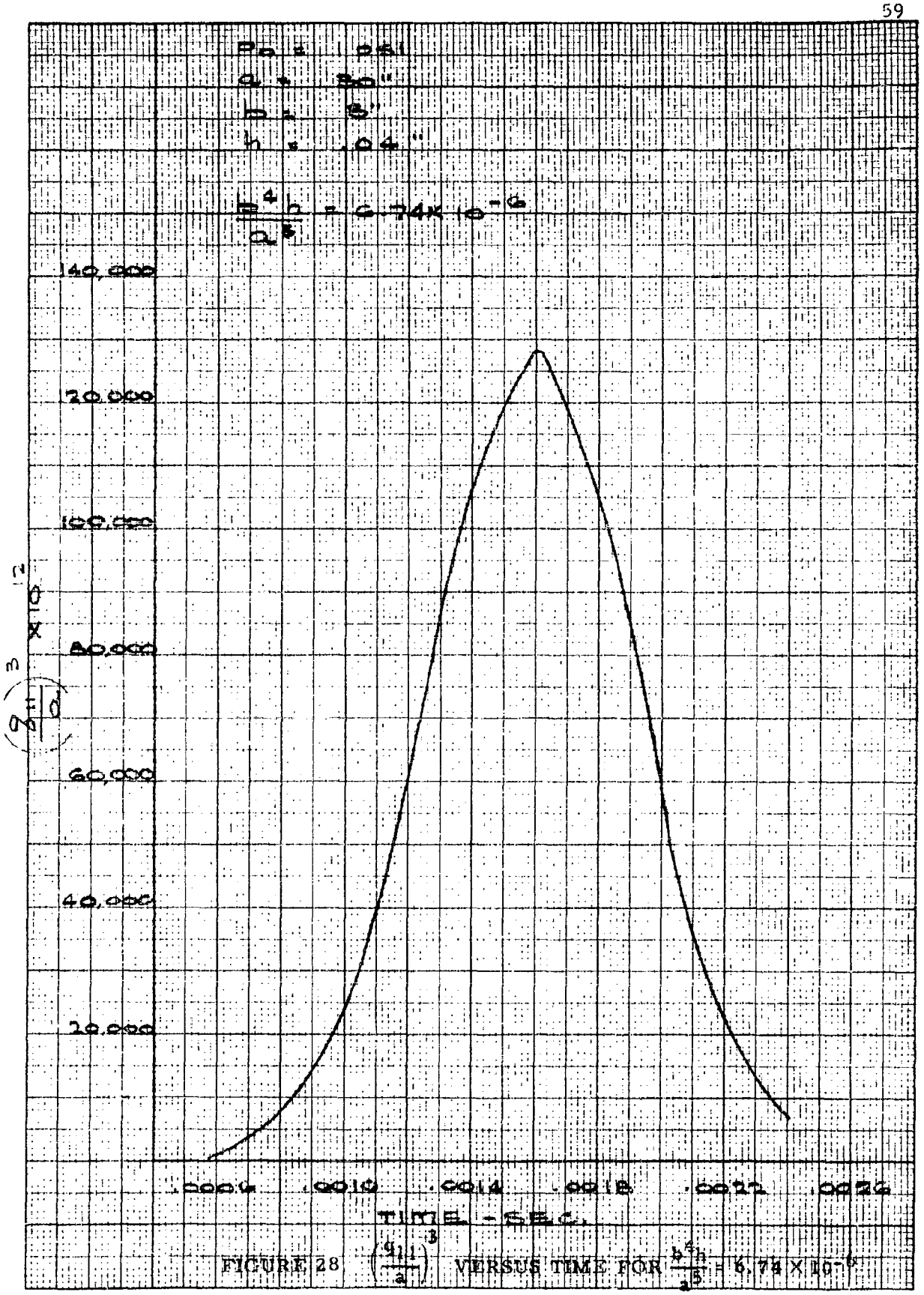

FIGURE 28 $\left(\frac{q_{1,1}}{a}\right)^3$ VERSUS TIME FOR $\frac{b^4 h}{a^5}$ = 6.74 X 10⁻⁶ AND P_o = 1 PSI

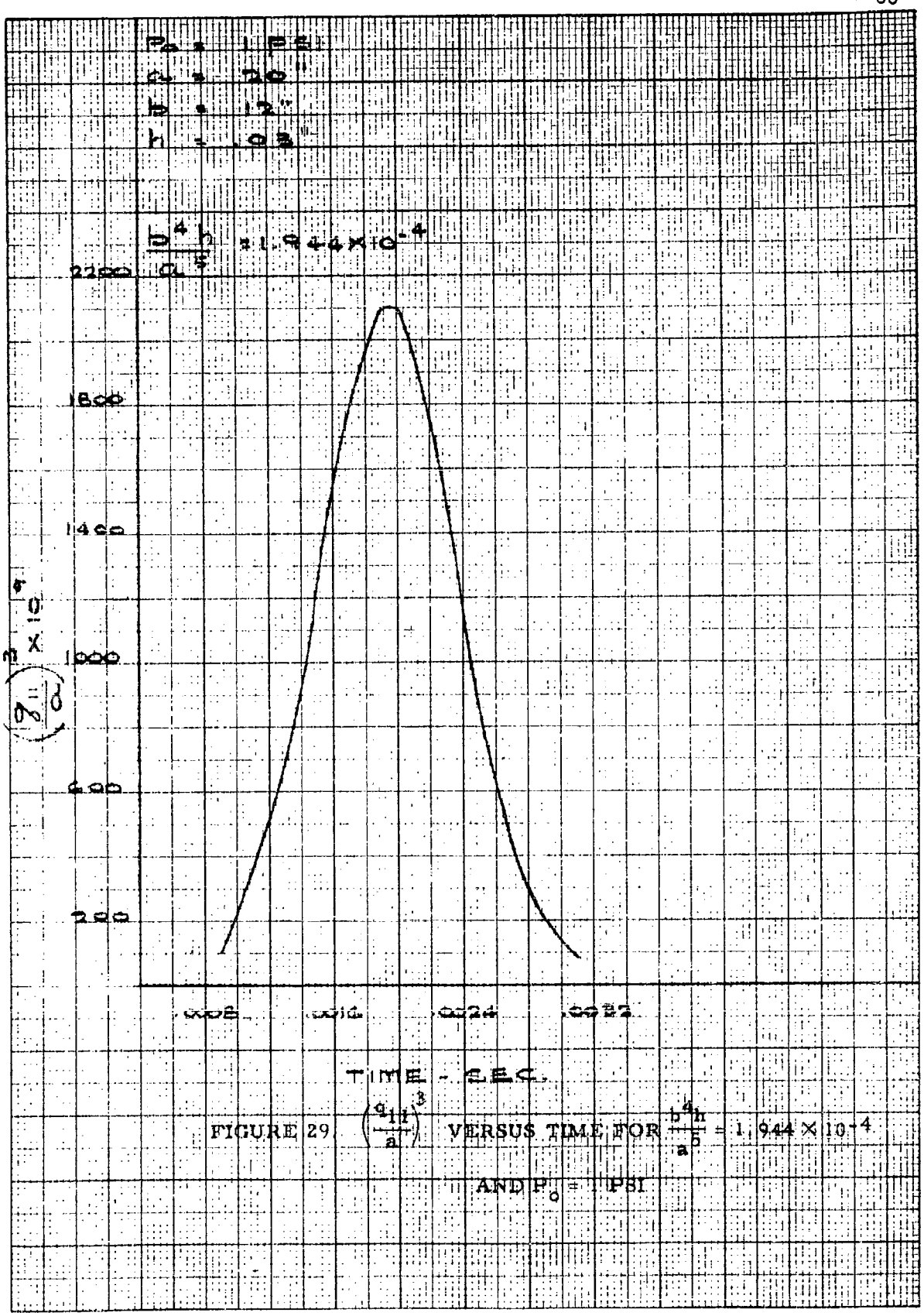

FIGURE 29 $\left(\frac{q_1 t}{a}\right)^3$ VERSUS TIME FOR $\frac{b^4 h}{a^5} = 1.944 \times 10^{-4}$ AND P_o = 1 PSI

The M = generalized mass, which for constant cross section is given by

$$M = m_i \int_{s|\theta=0}^{s|\theta=2\pi} \phi^2(s)\, ds \tag{42}$$

where

m_i = Mass per unit length of frame

The numerical integration of Equation (39) reduces to the difference equation

$$q(t_i + 1) = \frac{Q(t_i)}{M}(\Delta t)^2 + [2 - \omega^2(\Delta t)^2]\, q(t_i) - q(t_i - 1) \tag{43}$$

$$\text{with } q(0) = q(1) = 0$$

where

(Δt) = Time interval

Then the maximum bending stress is given by

$$\sigma\big|_{max} = M_{max} \cdot \frac{c}{I}$$

but

$$M_{max} = -EI \left.\frac{\partial^2 \Phi(s,t)}{\partial s^2}\right|_{max} = -EI \left.\frac{\partial^2 \psi(s)}{\partial s^2}\right|_{max} \cdot q_{max}(t)$$

or

$$\sigma\Big|_{max} = - Ec \left.\frac{\partial^2 \phi(s)}{\partial s^2}\right|_{max} \cdot q_{max}(t) \qquad (44)$$

K. Determination of the Dynamic Response of a Typical Elliptical Frame

The typical frame considered, with the attached stringers and skin, is given in Figure 30. Considering the loading coming from one side of the frame, due to intensity of 2 psi and with positive phase duration of 1 sec, the maximum bending stress was determined to be equal to $\sigma_d = 93,200$ psi.

L. Comparison of the Order of Magnitude of the Static and Dynamic Stresses and Additional Static Deflection Curves

The determination of the maximum bending moment in an elliptical ring under uniform static pressure is given by S. Timoshenko.* This moment, for the geometry considered in the previous case, is given by $0.870\ Pb^2$, where P is the uniform load intensity on the frame, and b is half of the minor axis of the ellipse.

If P = (2)(9) = 18 pli (i.e., half of the panel load per length of frame), then the maximum static bending stress would be

$$\sigma_{st} = M\frac{c}{I} = 0.870(18)(16)^2\frac{1.505}{0.147} = 41,000 \text{ psi}$$

*S. Timoshenko, "Strength of Materials," Part II, Second Edition, p. 90.

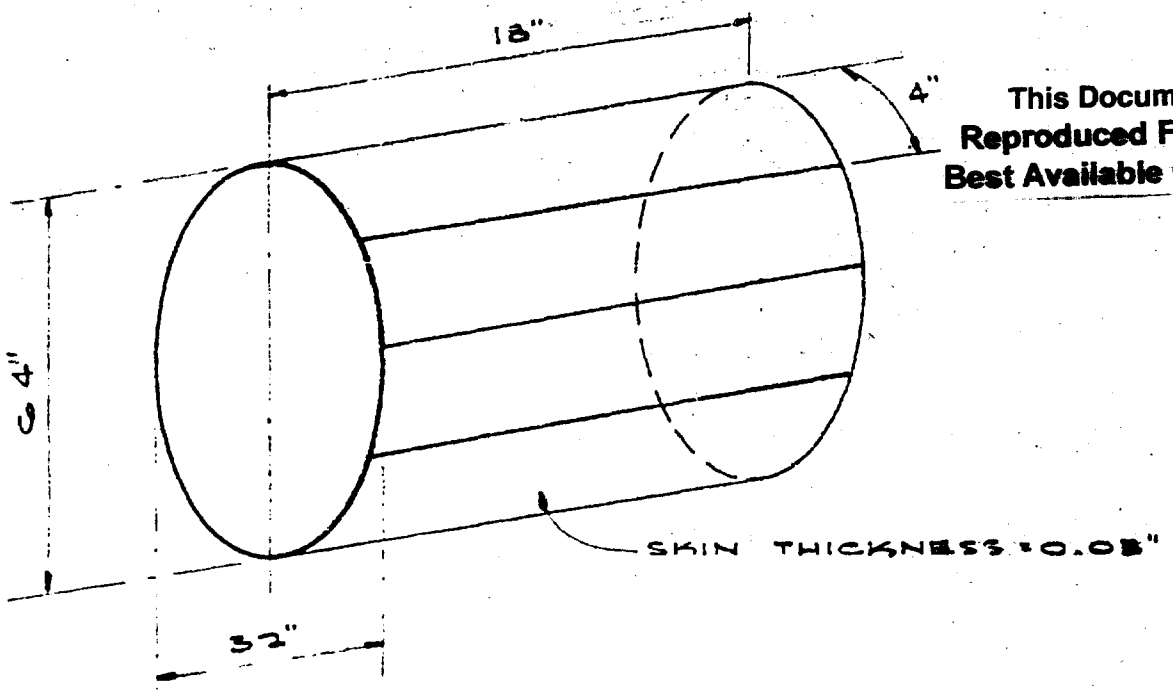

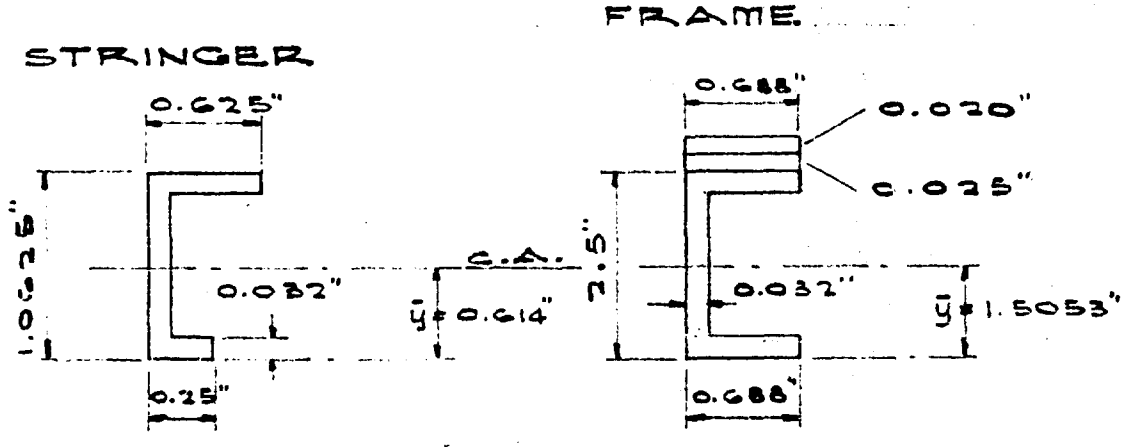

$A = 0.060$ in.^{2}
$I = 0.00950$ in.^{4}

$A = 0.152944$ in.^{2}
$I = 0.146931$ in.^{4}

FIGURE 30. TYPICAL FUSELAGE SECTION

The same frame was considered under uniform dynamic pressure of peak intensity P_o = 18 pli, and the maximum dynamic stress obtained was found equal to 73,000 psi. Thus, the ratio of the maximum dynamic to maximum static pressure for peak intensity equal to the static load intensity is equal to $\frac{73,000}{41,000}$ = 1.78. It should be observed that the frame under consideration is not loaded uniformly, and that most of the loading is a concentrated loading coming from the stringers' reactions. For such a loading, the σ_d would be greater than 73,000 psi, and, thus, compared with the dynamic bending stress obtained in the previous section (i.e., σ_d = 93,200 psi) results in a check on the order of magnitude of the obtained maximum dynamic bending stress.

Static deflection curves have been obtained for a/b equal to 2.5 and 1.666. They are given in Figures 31 and 32 and can be used for any a and b of the same ratio.

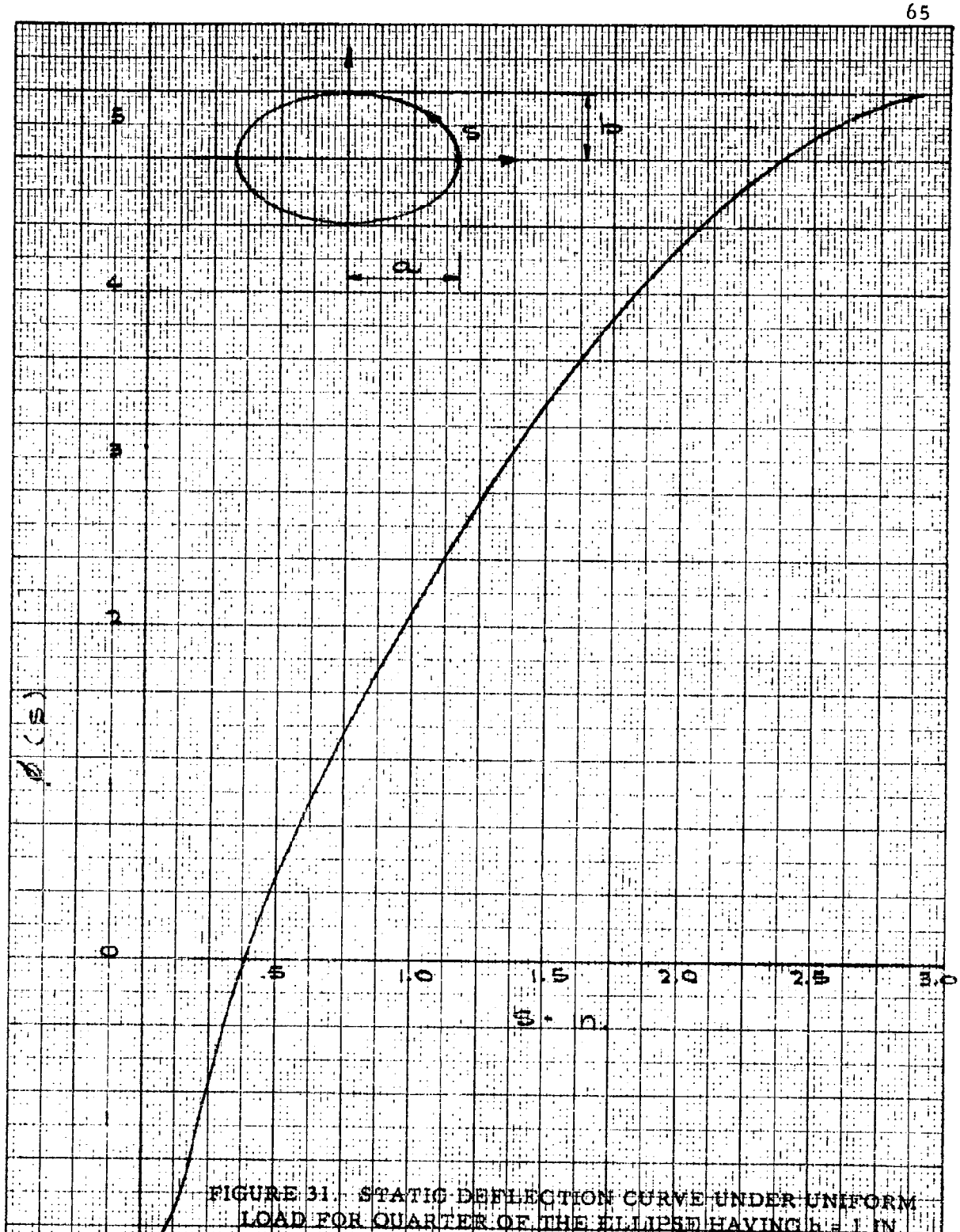

FIGURE 31. STATIC DEFLECTION CURVE UNDER UNIFORM LOAD FOR QUARTER OF THE ELLIPSE HAVING b = 1 IN. AND a/b = 2.5

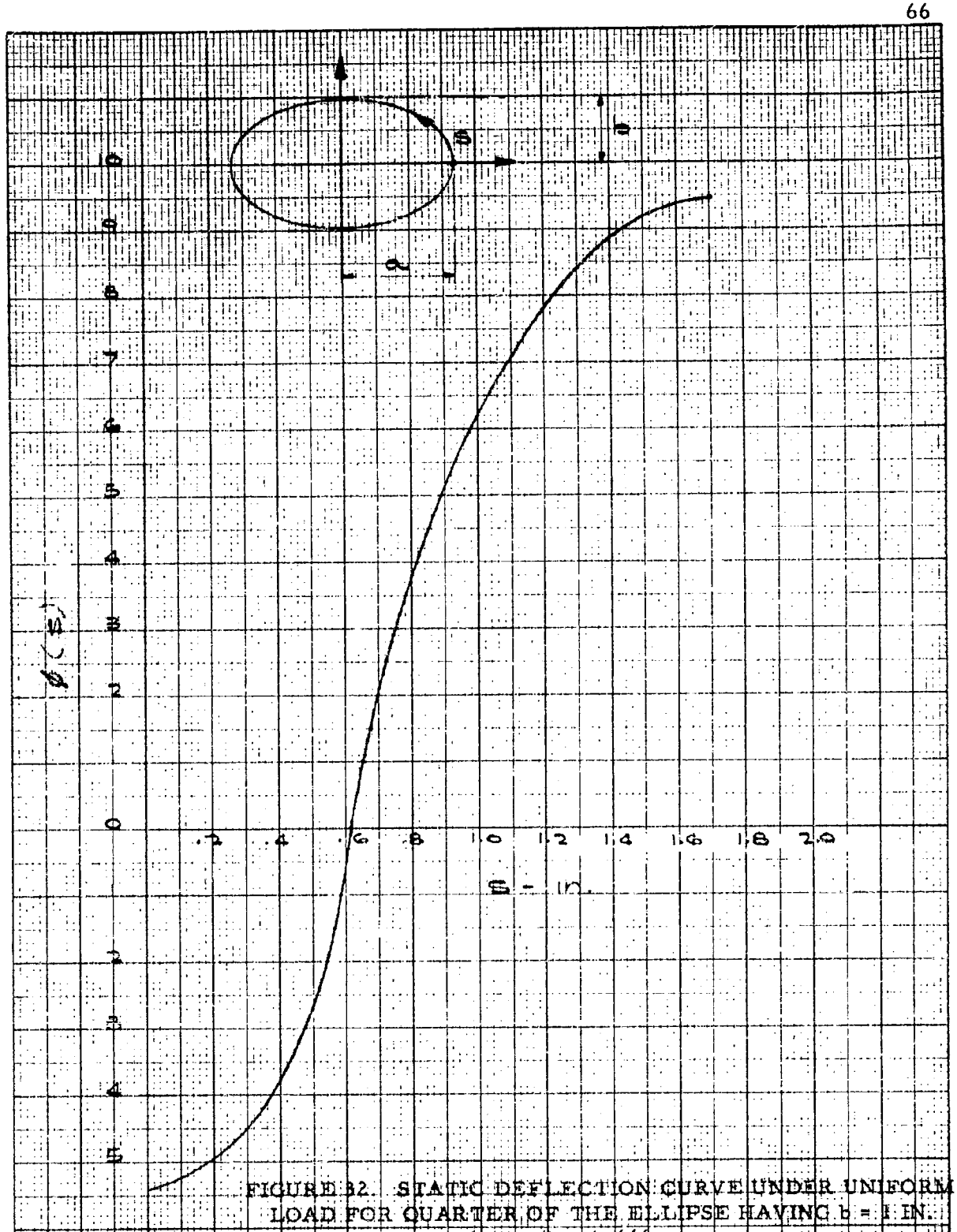

FIGURE 32. STATIC DEFLECTION CURVE UNDER UNIFORM LOAD FOR QUARTER OF THE ELLIPSE HAVING b = 1 IN. AND a/b = 1.666

M. Sample Calculations

In this section, the response of the skin, stringer, and frame shown in Figure 30 will be considered in detail for peak pressure intensity of P_o = 2 psi, and positive time duration t_+ = 1 sec.

1. Skin Response

The generalized coordinate of the skin response is governed by Equation (21) given below

$$q_{mn}(t_i + 1) = 2q_{mn}(t_i) + A_{mn}(t_i) + B_{mn}q^3_{mn}(t_i) - q_{mn}(t_i - 1)$$

where

$$A_{mn}(t_i) = \frac{1.624(\Delta t)^2 P_o}{m_i mn}\left(1 - \frac{t_i}{t_+}\right)$$

$$B_{mn} = -\frac{18.20Eh(\Delta t)^2}{m_i}\left[\frac{m^4}{a^4} + \frac{n^4}{b^4}\right]$$

For

$E = 10.6 \times 10^6$ psi

$h = 0.03$ in.

$P_o = 2$ psi

$\Delta t = 0.0001$ sec

$a = 18$ in.

$b = 4$ in.

The

$$m_i = 7.42 \times 10^{-6} \text{ lb in}^{-1} \text{ sec}^2$$

$$B_{11} = -30.5435$$

$$B_{13} = -2,468.068$$

$$B_{31} = -36.4877$$

$$B_{33} = -2,474.0196$$

The $A_{mn}(t_i)$ have been computed and are given in tabular form in Tables 1, 2, 3, and 4 where the numerical integration of Equation (21) is performed for the determination of the generalized coordinates $q_{mn}(t)$

The maximum stress in the skin is given by Equation (23)

$$\sigma_{max} = \left\{ \Sigma\Sigma 2.46E\left(\frac{n}{b}\right)^2 q_{mn}^2(t) \right\}_{max}$$

or, using the results obtained in Tables 1, 2, 3, and 4, the

$$\sigma_{max} = \frac{2.46(10.6 \times 10^6)}{(4)^2} \left\{ (0.08376)^2 + (3)^2 (0.00523)^2 + (0.03865)^2 \right.$$

$$\left. + (3)^2 (0.009306)^2 \right\} = 15,600 \text{ psi}$$

2. Stringer Response

The generalized coordinate of the stringer response is given by Equation (35)

$$q_i(t_i + 1) = A_i(t_i) + B_i q_i(t_i) - q_i(t_i - 1)$$

TABLE I. DETERMINATION OF $q_{11}(t)$

t-sec	(1) $A_{11}(t_i)$	(2) $q_{11}(t_i)$	(3) $2q_{11}(t_i)$	(4) $q_{11}^3(t_i)$	(5) -30.5435 (4)	(6) $q_{11}(t_i - 1)$	(7) = (1) + (3) + (5) - (6) $q_{11}(t_i + 1)$
0	0.004374	0	0	0	0	0	0.004374
0.0001	0.004374	0.004374	0.008748	8.3683×10^{-8}	2.5559×10^{-6}	0	0.013119
0.0002	0.004374	0.013119	0.026238	2.2579×10^{-6}	6.8964×10^{-5}	0.004374	0.02617
0.0003	0.004374	0.02617	0.05234	1.7923×10^{-5}	5.4743×10^{-4}	0.013119	0.04305
0.0004	0.004374	0.04305	0.08610	7.9785×10^{-5}	2.437×10^{-3}	0.02617	0.06187
0.0005	0.004374	0.06187	0.12374	2.3603×10^{-4}	7.23365×10^{-3}	0.04305	0.07783
0 0006	0.004374	0.07783	0.15566	4.71456×10^{-4}	1.43999×10^{-2}	0.06187	0.08373
0.0007	0.004374	0.08376	0.16752	5.876×10^{-4}	1.7947×10^{-2}	0.07783	0.076117
0.0008	0.004374	0.076117	0.15223	4.41006×10^{-4}	1.3470×10^{-2}	0.08376	0.05937
0.0009	0.004374	0.05937	0.1187	2.0927×10^{-4}	6.3918×10^{-3}	0.076117	0.04057
0.0010	0.004374	0.04057	0.08114	6.6775×10^{-5}	2.03954×10^{-3}	0.05937	0.02410
0.0011	0.004374	0.02410	0.0482	1.3997×10^{-5}	4.27517×10^{-4}	0.04057	0.011576
0.0012	0.004374	0.011576	0.02315	1.5512×10^{-6}	4.73786×10^{-5}	0.02410	0.003377

TABLE 2. DETERMINATION OF $q_{13}(t)$

t-sec	(1) $A_{13}(t_i)$	(2) $q_{13}(t_i)$	(3) $2q_{13}(t_i)$	(4) $q_{13}^3(t_i)$	(5) $-2,468.068\ (4)$	(6) $q_{13}(t_i - 1)$	(7) = (1) + (3) + (5) - (6) $q_{13}(t_i + 1)$
0	0.001458	0	0	0	0	0	0.001458
0.0001	0.001458	0.001458	0.002916	3.0994×10^{-9}	7.6495×10^{-6}	0	0.004367
0.0002	0.001458	0.004367	0.008734	8.32817×10^{-8}	2.0554×10^{-4}	0.001458	0.008529
0.0003	0.001458	0.008529	0.017058	6.2043×10^{-7}	1.5313×10^{-3}	0.004367	0.01262
0.0004	0.001458	0.01262	0.02524	2.0099×10^{-6}	4.9606×10^{-3}	0.008529	0.01321
0.0005	0.001458	0.01321	0.02642	2.3051×10^{-6}	5.6893×10^{-3}	0.01262	0.009569
0.0006	0.001458	0.009569	0.01914	8.762×10^{-7}	2.1625×10^{-3}	0.01321	0.00523
0.0007	0.001458	0.00523					

TABLE 3. DETERMINATION OF $q_{31}(t)$

t-sec	(1) $A_{31}(t_i)$	(2) $q_{31}(t_i)$	(3) $2q_{31}(t_i)$	(4) $q_{31}^3(t_i)$	(5) $-36.4877\ (4)$	(6) $q_{31}(t_i - 1)$	(7) = (1) + (3) + (5) - (6) $q_{31}(t_i + 1)$
0	0.001458	0	0	0	0	0	0.001458
0.0001	0.001458	0.001458	0.002916	3.0994×10^{-9}	1.1309×10^{-7}	0	0.004374
0.0002	0.001458	0.004374	0.008748	8.3683×10^{-8}	3.0534×10^{-6}	0.001458	0.008745
0.0003	0.001458	0.008745	0.017490	6.6877×10^{-7}	2.4403×10^{-5}	0.004374	0.01455
0.0004	0.001458	0.01455	0.02910	3.0803×10^{-6}	1.1239×10^{-4}	0.008745	0.02170
0.0005	0.001458	0.02170	0.04340	1.0218×10^{-5}	3.7283×10^{-4}	0.01455	0.02994
0.0006	0.001458	0.02994	0.05988	2.6838×10^{-5}	9.7926×10^{-4}	0.02170	0.03865
0.0007	0.001458	0.03865					

TABLE 4. DETERMINATION OF $q_{33}(t)$

t-sec	(1) $A_{33}(t_i)$	(2) $q_{33}(t_i)$	(3) $2q_{33}(t_i)$	(4) $q_{33}^3(t_i)$	(5) $-2,474.096\ (4)$	(6) $q_{33}(t_i - 1)$	(7) = (1) + (3) + (5) - (6) $q_{33}(t_i + 1)$
0	0.000486	0	0	0	0	0	0.000486
0.0001	0.000486	0.000486	0.000972	1.1478×10^{-10}	2.8397×10^{-7}	0	0.0014577
0.0002	0.000486	0.0014577	0.002915	3.0975×10^{-9}	7.6632×10^{-6}	0.000486	0.002908
0.0003	0.000486	0.002908	0.005816	2.4592×10^{-8}	6.0841×10^{-5}	0.0014577	0.004783
0.0004	0.000486	0.004783	0.009566	1.0942×10^{-7}	2.70707×10^{-4}	0.002908	0.006873
0.0005	0.000486	0.006873	0.013746	3.2467×10^{-7}	8.0324×10^{-4}	0.004783	0.008646
0.0006	0.000486	0.008646	0.017292	6.4632×10^{-7}	1.599×10^{-3}	0.006873	0.009306
0.0007	0.000486	0.009306					

where

$$A_i(t_i) = \frac{7.74Eh}{m_i a_i} \beta_i \left(\frac{q_{11}(t_i)}{b}\right)^3 (\Delta t)^2$$

and

$$B_i = [2 - \omega_i^2 (\Delta t)^2]$$

The $A_i(t)$ are practically proportional to β_i and thus the $A_2(t)$ is negligible compared to $A_1(t)$. The $A_1(t)$ and $A_2(t)$, as well as the B_1 and B_2, are computed and given in Tables 5 and 6 with the numerical integration of Equation (35) for the determination of $q_1(t)$ and $q_3(t)$. The $q_1(t)$ and $q_3(t)$ are given in Tables 5 and 6, and it is clearly shown that the contribution of $q_3(t)$ in determining the dynamic response of the stringer can be neglected, and, by doing that, the response obtained is slightly on the conservative side.

Thus, the maximum bending moment and shear at $x = 0$ as given by Equations (36) and (37) reduce to

$$M_{max} = -\frac{2EI}{a^2} q_{1\,max}(t)(k_1 a)^2 \lambda_1 \tag{45}$$

and

$$V\Big|_{\substack{max \\ x=0}} = \frac{2EI}{a^3} q_{1\,max}(t)(k_1 a)^3 \tag{46}$$

TABLE 5. DETERMINATION OF $q_1(t)$

t-sec	$\left(\frac{q_{1\,1}(t_i)}{b}\right)^3$	(1) $A_1(t_i)$	(2) $q_1(t_i)$	(3) 1.675 (2)	(4) $q_1(t_i - 1)$	(5) = (1) + (3) - (4) $q_1(t_i + 1)$
0	0×10^{-6}	0×10^{-6}	0×10^{-6}	0×10^{-6}	0×10^{-6}	0×10^{-6}
0.0001	0.0012	0.7022	0	0	0	0.7022
0.0002	0.03525	20.627	0.7022	1.1762	0	21.803
0.0003	0.2801	163.9067	21.8032	36.5204	0.7022	199.725
0.0004	1.2458	729.6073	199.725	334.539	21.803	1,041.744
0.0005	3.7023	2,166.482	1,041.744	1,744.921	199.725	3,711.678
0.0006	7.366	4,310.377	3,711.678	6,217.661	1,041.744	9,485.694
0.0007	9.1822	5,373.166	9,485.694	15,838.54	3,711.678	17,550.03
0.0008	6.8915	4,032.713	17,550.03	29,396.3	9,485.694	23,943.3
0.0009	3.2682	1,912.459	23,943.3	40,105.18	17,550.03	24,467.6
0.0010	1.0426	610.1003	24,4676	40,983.2	23,943.3	17,650.00

TABLE 6. DETERMINATION OF q_3 (t)

t-sec	(1) $A_3(t_i)$	(2) $q_3(t_i)$	(3) 1.6207 (2)	(4) $q_3(t_i - 1)$	(5) = (1) + (3) - (4) $q_3(t_i + 1)$
0	0×10^{-6}	0×10^{-6}	0×10^{-6}	0×10^{-6}	0×10^{-6}
0.00020	0.2544	0	0	0	0.2594
0.00022	0.44	0.2594	0.4204	0	0.8604
0.00024	0.64	0.8604	1.394	0.2594	1.7751
0.00026	0.84	1.7751	2.877	0.8604	2.857
0.00028	1.04	2.857	4.6303	1.7751	3.895
0.00030	1.206	3.895	6.3126	2.857	4.6616
0.00032	2.000	4.6616	7.555	3.895	5.6600
0.00034	3.2	5.6600	9.1732	4.6616	7.7116
0.00036	4.6	7.7116	12.4982	5.6600	11.4381
0.00038	6.8	11.4381	18.5377	7.7116	17.6261
0.00040	9.16	17.6261	28.5666	11.4381	26.289
0.00042	12.00	26.289	42.6066	17.6261	36.9805
0.00044	14.80	36.9805	59.934	26.289	48.445
0.00046	18.40	48.445	78.5148	36.9805	59.934
0.00048	22.40	59.934	97.135	48.445	71.090
0.00050	27.25	71.090	115.216	59.934	82.532
0.00052	32.80	82.532	133.760	71.090	95.470
0.00054	38.4	95.470	154.728	82.532	110.596
0.00056	43.2	110.596	179.243	95.470	126.973
0.00058	49.2	126.973	205.785	110.596	144.389
0.00060	54.21	144.389	234.011	126.973	161.248
0.00062	58.40	161.248	261.335	144.389	175.345
0.00064	62.4	175.345	284.1816	161.248	185.334
0.00066	64.8	185.334	300.371	175.345	189.826
0.00068	67.2	189.826	307.691	185.334	139.517
0.00070	67.6	189.517	307.150	189.826	184.924

For the case under consideration, the

$$M_{max} = -\frac{2(10.6 \times 10^6)\, I\, (0.0244)(4.73)^2 (-1.0175)}{(18)^2} = 364 \times 10^2\, I$$

$$\sigma_{max} = \frac{Mc}{I} = 364 \times 10^2 (0.614) = 22,300 \text{ psi}$$

(from the loading of one panel)

and

$$V\Big|_{\substack{x=0 \\ max}} = \frac{2(10.6 \times 10^6)}{(18)^3} (0.0095)(0.0244)(4.73)^3 = 89.6 \text{ lb}$$

(from the loading of one panel)

3. Frame Response

For the frame under consideration, the mode shape to be used has been determined and given in Figure 33. Obtaining $(q_{11}/a)^3$ from Figure 24, $q_1(t)$ from Table 5, using the mode given in Figure 33, and using numerical integration, the w, Q(t) and M given by Equations (40), (41) and (42) have been computed, and then Equation (43) was integrated to determine the generalized coordinate q(t).

The numerical integration of Equation (43) is given in tabular form in Table 7. Then the maximum bending stress is given by the Equation (44):

FIGURE 33 STATIC DEFLECTION
THE ELLIPSE FOR THE FRAME CO

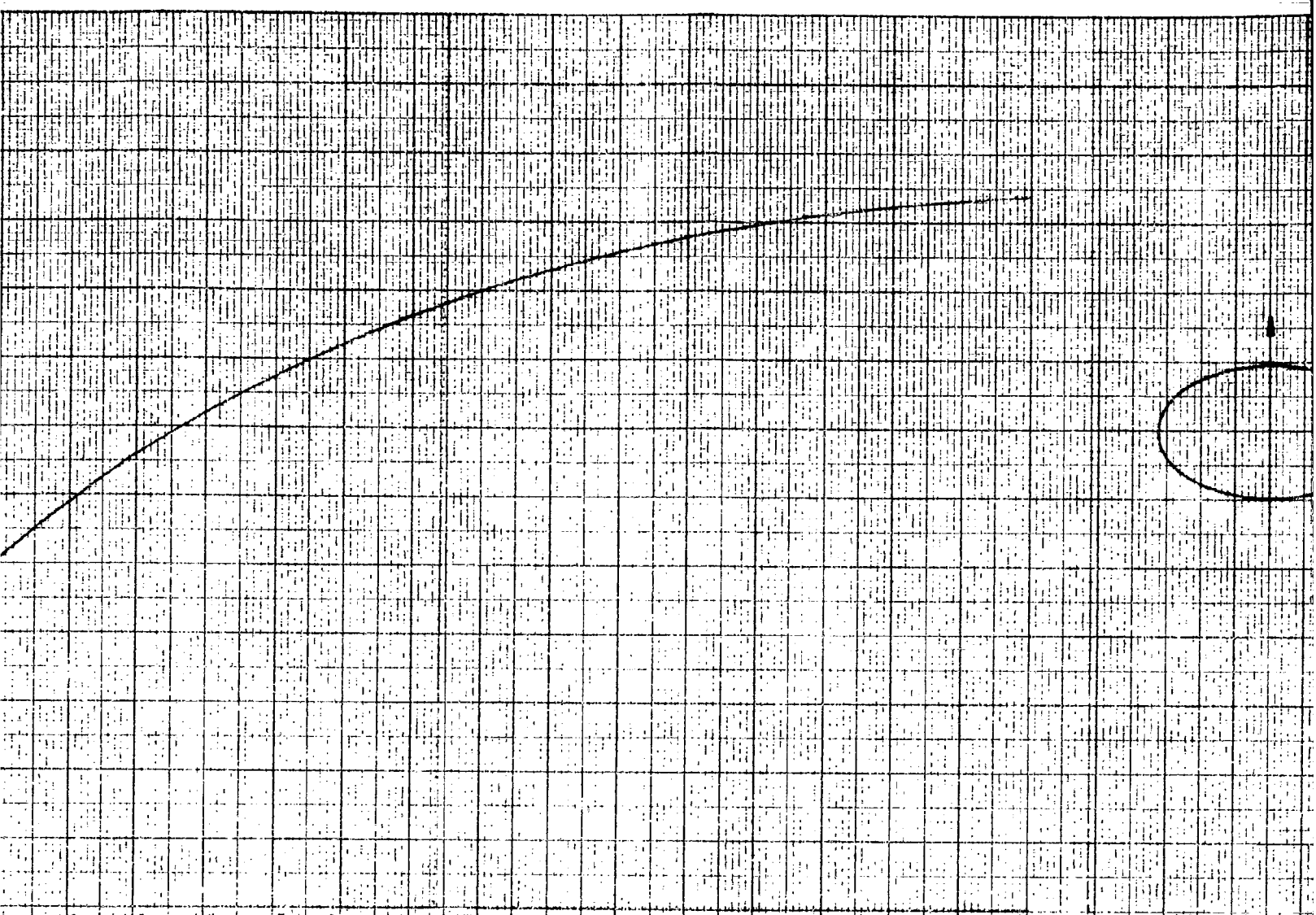

2

FIGURE 33. STATIC DEFLECTION CURVE, $\phi(s)$, FOR QUARTER OF THE ELLIPSE FOR THE FRAME CONSIDERED UNDER UNIFORM LOAD

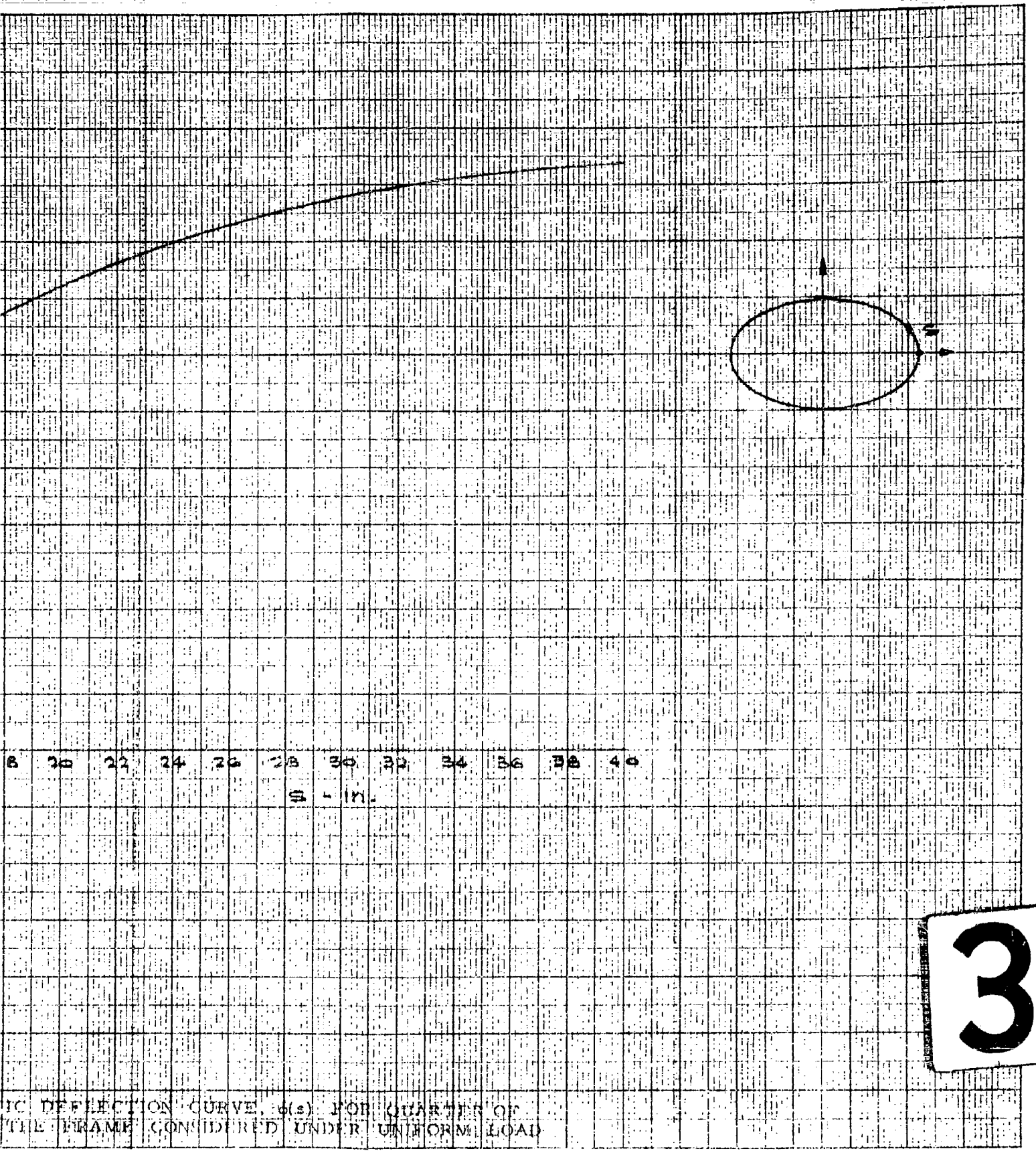

3

IC DEFLECTION CURVE, $\phi(s)$ FOR QUARTER OF THE FRAME CONSIDERED UNDER UNIFORM LOAD

TABLE 7. DETERMINATION OF q(t)

t-sec	(1) $\frac{Q(t_i)}{M}(\Delta t)^2$	(2) $q(t_i)$	(3) $[2 - \omega^2(\Delta t)^2](2)$	(4) $q(t_i - 1)$	(5) = (1) + (3) - (4) $q(t_i + 1)$
0	0×10^{-7}	0×10^{-7}	0×10^{-7}	0×10^{-7}	0×10^{-7}
0.0001	16.88	0	0	0	16.88
0.0002	528.25	16.88	30.7216	0	558.9716
0.0003	4,839.8	558.9716	1,017.33	16.88	5,840.25
0.0004	25,739.8	5,840.25	10,629.255	558.9716	35.310.08
0.0005	229,823.6	35,310.08	64,264.34	5,840.25	288,247.7
0.0006	425,215.3	288,247.7	524,610.9	35,310.08	914,516.13
0.0007	580,107.4	914,515.13	1,664,419.	228,247.71	1,956,279.0
0.0008	592,810.4	1,956,279.0	3,560,427.7	914,516.13	3,238,772.
0.0009	427,631.6	3,238,722	5,894,474.	1,956,279.	4,365,826.7
0.0010	218,750.0	4,365,867.7	7,945,879.2	3,238,722	4,925,907
0.0011	93,750.	4,925,907.	8,965,151.1	4,365,826.7	4,693,074.

$$\sigma_{max} = - Ec \left.\frac{\partial^2 \phi(s)}{\partial s^2}\right|_{max} \cdot q_{max}(t)$$

The $\frac{\partial^2 \phi(s)}{\partial s^2}$ is maximum at s = 0. The origin of the curve on Figure 33 has been replotted in larger scale and is given in Figure 34. Numerical differentiation yields

$$\frac{\partial^2 \phi(o)}{\partial s^2} = \frac{2\phi(\Delta s) - 2\phi(o)}{(\Delta s)^2} = \frac{2(-0.080) - 2(-0.0825)}{(0.65)^2} = 0.01185$$

Then

$$\sigma_{max} = 10.6 \times 10^6 (1.505)(0.01185)(0.4925) = 93,200 \text{ psi}$$

(from the loading of one side of the frame)

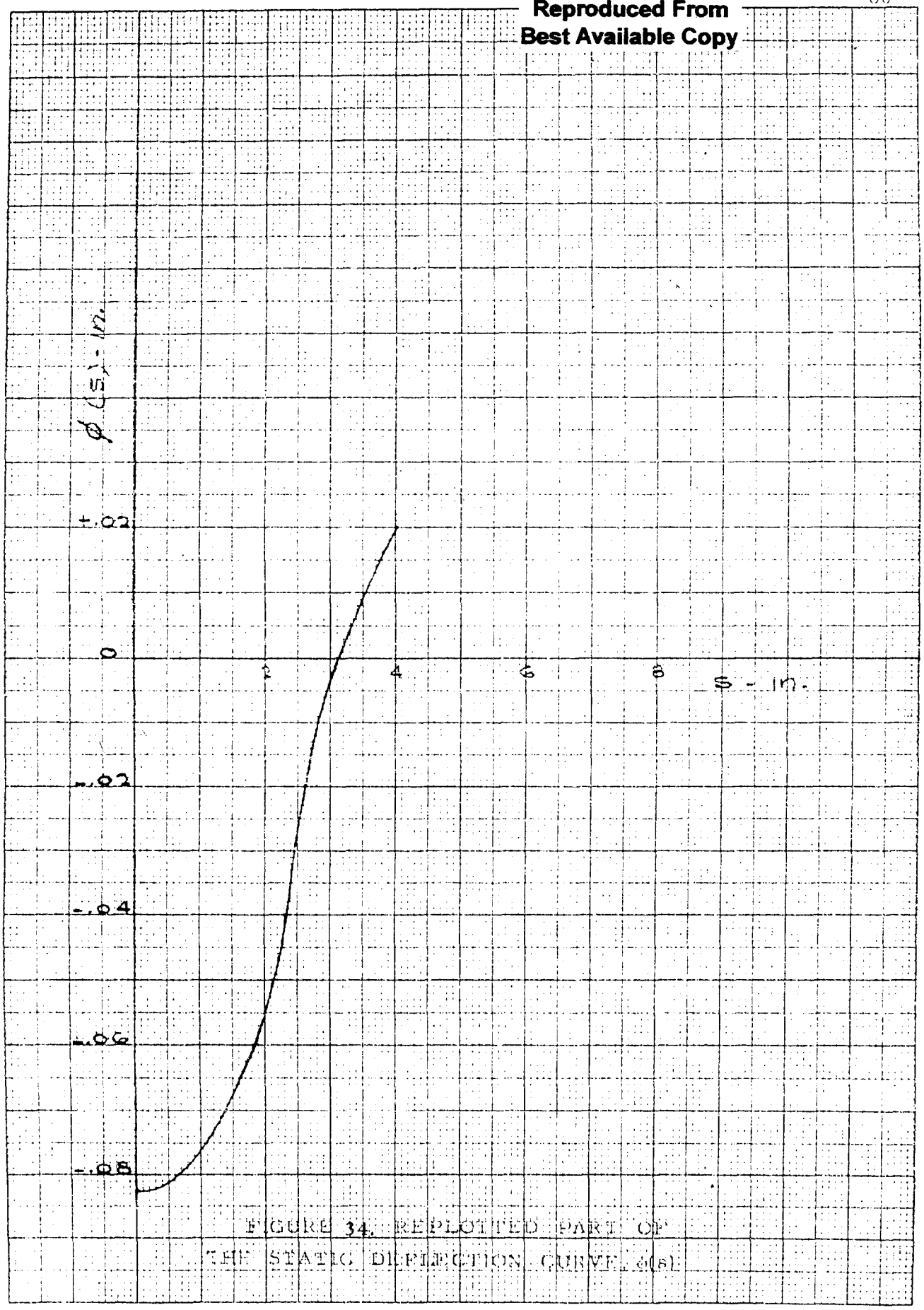

FIGURE 34. REPLOTTED PART OF THE STATIC DEFLECTION CURVE [68]